



Early View

Original research article

***Rothia mucilaginosa* is an anti-inflammatory bacterium in the respiratory tract of patients with chronic lung disease**

Charlotte Rigauts, Juliana Aizawa, Steven Taylor, Geraint B. Rogers, Matthias Govaerts, Paul Cos, Lisa Ostyn, Sarah Sims, Eva Vandeplassche, Mozes Sze, Yves Dondelinger, Lars Vereecke, Heleen Van Acker, Jodie L. Simpson, Lucy Burr, Anne Willems, Michael M. Tunney, Cristina Cigana, Alessandra Bragonzi, Tom Coenye, Aurélie Crabbé

Please cite this article as: Rigauts C, Aizawa J, Taylor S, *et al.* *Rothia mucilaginosa* is an anti-inflammatory bacterium in the respiratory tract of patients with chronic lung disease. *Eur Respir J* 2021; in press (<https://doi.org/10.1183/13993003.01293-2021>).

This manuscript has recently been accepted for publication in the *European Respiratory Journal*. It is published here in its accepted form prior to copyediting and typesetting by our production team. After these production processes are complete and the authors have approved the resulting proofs, the article will move to the latest issue of the ERJ online.

***Rothia mucilaginosa* is an anti-inflammatory bacterium in the respiratory tract of patients with chronic lung disease.**

Charlotte Rigauts¹, Juliana Aizawa², Steven Taylor³, Geraint B. Rogers³, Matthias Govaerts², Paul Cos², Lisa Ostyn¹, Sarah Sims³, Eva Vandeplassche¹, Mozes Sze⁴, Yves Dondelinger^{4,5}, Lars Vereecke^{4,6}, Heleen Van Acker¹, Jodie L. Simpson⁷, Lucy Burr^{8,9}, Anne Willems¹⁰, Michael M. Tunney¹¹, Cristina Cigana¹², Alessandra Bragonzi¹², Tom Coenye¹, Aurélie Crabbé^{1*}

¹Laboratory of Pharmaceutical Microbiology, Ghent University, Belgium.

²Laboratory of Microbiology, Parasitology and Hygiene, University of Antwerp, Wilrijk, Belgium.

³Microbiome and Host Health Programme, the South Australian Health and Medical Research Institute (SAHMRI), Adelaide, South Australia, Australia; The SAHMRI Microbiome Research Laboratory, School of Medicine, Flinders University, Adelaide, South Australia, Australia.

⁴VIB Center for Inflammation Research, Ghent, Belgium.

⁵Department of Biomedical Molecular Biology, Ghent University, Belgium.

⁶Department of Rheumatology, Ghent University, Belgium.

⁷Faculty of Health and Medicine, Priority Research Centre for Healthy Lungs, University of Newcastle, New South Wales, Australia.

⁸Department of Respiratory Medicine, Mater Health Services, South Brisbane, QLD, Australia

⁹Mater Research - University of Queensland, Aubigny Place, South Brisbane, QLD, Australia

¹⁰Laboratory of Microbiology, Department of Biochemistry and Microbiology, Ghent University, Belgium.

¹¹School of Pharmacy, Queen's University Belfast, Belfast, United Kingdom.

¹²Infections and Cystic Fibrosis Unit, Division of Immunology, Transplantation and Infectious Diseases, IRCCS San Raffaele Scientific Institute, Milan, Italy.

* Corresponding author: Ottergemsesteenweg 460, 9000 Ghent, Belgium;
aurelie.crabbe@ugent.be; +32 9 264 81 42

Take home message

A commensal bacterium of the lower airways, *Rothia mucilaginosa*, inhibits inflammation by NF-κB pathway inactivation. *R. mucilaginosa* abundance inversely correlates with sputum pro-inflammatory markers in chronic lung disease, indicating a beneficial role.

Abstract

Chronic airway inflammation is the main driver of pathogenesis in respiratory diseases, such as severe asthma, chronic obstructive pulmonary disease (COPD), cystic fibrosis (CF), and bronchiectasis. While the role of common pathogens in airway inflammation is widely recognized, the influence of other microbiota members is still poorly understood. Here, we show that *Rothia mucilaginosa*, a common resident of the oral cavity that is also often detectable in the lower airways in chronic disease, has an inhibitory effect on pathogen- and LPS-induced pro-inflammatory responses, both *in vitro* (3-D cell culture model) and *in vivo* (mouse model). Furthermore, in a cohort of adults with bronchiectasis, the abundance of *Rothia* spp. was negatively correlated with pro-inflammatory markers (IL-8, IL-1 β) and matrix metalloproteinases (MMP-1, MMP-8 and MMP-9) in sputum. Mechanistic studies revealed that *R. mucilaginosa* inhibits NF- κ B pathway activation by reducing the phosphorylation of I κ B- α and consequently the expression of NF- κ B target genes. These findings indicate that the presence of *R. mucilaginosa* in the lower airways potentially mitigates inflammation, which could in turn influence severity and progression of chronic respiratory disorders.

Introduction

Persistent or dysregulated lung inflammation is a hallmark of chronic respiratory diseases, such as severe asthma, chronic obstructive pulmonary disease (COPD), cystic fibrosis (CF) and bronchiectasis [1–9]. In patients with chronic airway disease, the release of pro-inflammatory cytokines by cells of the lung mucosa in response to external triggers (pathogenic microorganisms, cigarette smoke, pollutants or allergens) typically leads to infiltration of innate immune cells, such as neutrophils or eosinophils, that further exacerbate lung inflammation [5–7, 10, 11]. Persistent inflammation and associated tissue damage impairs lung clearance and facilitates the accumulation of microbes in the lower airways. These microbes represent both recognized respiratory pathogens and oropharyngeal commensal taxa that originate in the upper airways [12].

Colonization of the lower airways by specific bacterial and fungal species contributes directly to inflammation, tissue damage and lung disease progression [13–15]. These include *Pseudomonas aeruginosa* and *Staphylococcus aureus* in patients with CF [16–18], *Haemophilus influenzae* and *P. aeruginosa* in patients with bronchiectasis [19], *H. influenzae* in patients with neutrophilic asthma [20], and *Moraxella catarrhalis* in patients with COPD [21]. The presence and abundance of these pathogens is largely viewed as the sole microbial determinant of airway disease. However, in addition to these pathogens, the lower airways of patients with chronic lung disease are also colonized by a much wider microbiota that includes many bacterial taxa that are not considered to contribute directly to pathogenesis [12, 14, 22–24].

The composition of this wider airway microbiota differs with disease characteristics, severity, and patient age [25–27]. Yet, the potential of microbiota members to influence disease by mediating or moderating the impact of pro-inflammatory external triggers, including airway pathogens, is little understood [28–30].

We hypothesized that the lung microbiota contains bacteria with immunomodulatory activity which modulate net levels of immune activation by key respiratory pathogens, such as *P. aeruginosa*. Therefore, we assessed the immunomodulatory effect of several members of the lung microbiota, frequently reported as present in CF lower respiratory tract samples [31–33]. These species represented recognized pathogens (*S. aureus*), less frequently recovered pathogens (*Achromobacter xylosoxidans*, *Streptococcus anginosus*), and upper respiratory tract commensals thought to be broadly non-pathogenic in this context (*Rothia mucilaginosa* *Gemella haemolysans*). The latter includes the Gram-positive coccus, *R. mucilaginosa*, a common commensal of the oral cavity that is frequently detected in the lungs of patients with chronic lung disease [23, 34–37], and has been shown to be metabolically active and adapt to the CF lung environment [38]. We found that *R. mucilaginosa* exhibits anti-inflammatory activity *in vitro*. We subsequently validated our findings in an animal model of lung inflammation and in a cohort of patients with neutrophilic airways disease. Finally, we identified the host pathway that *R. mucilaginosa* interferes with to exert its anti-inflammatory effect.

Methods

Bacterial species and culturing conditions.

Six bacterial species (Table 1) commonly isolated from the CF lung were selected for this study, including two pathogens (*P. aeruginosa* and *S. aureus*), two less frequently recovered pathogens (*Streptococcus anginosus* and *Achromobacter xylosoxidans*) and two bacteria that are not typically considered as pathogens (*Rothia mucilaginosa* and *Gemella haemolysans*). Selective media for these species were previously developed [39, 40]. For select experiments we also included additional *Rothia* species, i.e. *R. dentocariosa*, *R. terrae*, *R. amarae* and *R. aeria*. All isolates were cultured at 37 °C under constant shaking conditions (250 rpm) in Brain Heart Infusion (BHI) broth (Lab M, Lancashire, UK) until

stationary phase. Most isolates were cultured in aerobic conditions except for *S. anginosus* and *G. haemolysans*, which were cultured in microaerobic conditions (<1% O₂) (Campygen Compact system, Oxoid, Thermo Fischer Scientific).

3-D lung epithelial cell culture models.

A549 cell line. A previously developed organotypic three-dimensional (3-D) cell culture model was used to study the immune response to pro-inflammatory stimuli [41–44]. 3-D *in vivo*-like lung epithelial cell culture model systems reflect key aspects of the parental tissue, including 3-D architecture, barrier function, apical-basolateral polarity, and multicellular complexity [41, 43]. It has been demonstrated that *P. aeruginosa* adhesion, as well as host-secreted cytokine profiles, in 3-D cell culture models of lung epithelial cells are more similar to the *in vivo* situation than cells grown as a monolayer on plastic [42]. A 3-D model of the human adenocarcinoma alveolar lung epithelial cell line A549 (ATCC CCL-185) was generated in GTSF-2 medium (HyClone, Logan, UT) supplemented with 1.5 g/L sodium bicarbonate (Sigma-Aldrich), 10% fetal bovine serum (FBS, Life technologies), 2.5 mg/L insulin transferrin sodium selenite (Lonza) and 1% penicillin-streptomycin (Life Technologies) at 37 °C under 5% CO₂. 3-D A549 cells were cultured for 11 to 14 days and were transferred to 48-well plates at a concentration of 2.5 x 10⁵ cells/well containing fresh serum-free GTSF-2 medium on the day of the infection.

IB-3 and S9 cell lines. The above-mentioned 3-D cell culture model was optimized for use with the IB-3 and S9 cell lines [45]. The IB-3 cell line is a bronchial epithelial cell line heterogeneous for F508del (F508del/W1282X). The S9 cell line originates from the IB-3 cell line and is stably transduced with wild-type Cystic Fibrosis Transmembrane Conductance Regulator (CFTR). LHC-8 medium without gentamicin (Life Technologies) supplemented with 5% FBS and 1% penicillin-streptomycin was used to culture both cell lines. The 3-D models of IB-3 and S9 cells were generated as described for the 3-D A549 model, except that a cell to bead ratio of 4:1 was used (as compared to 2:1 for the 3-D A549 model).

***In vitro* infection studies.** Prior to infection, bacterial cultures were centrifuged and resuspended in serum-free host cell culture medium. Cells were infected with single bacterial cultures for 4h at a multiplicity of infection (MOI) of 10:1, unless indicated otherwise. Additionally, cells were infected with *P. aeruginosa* together with each one of the CF lung microbiota members for 4h at a 10:1 ratio, resulting in an MOI of 20:1. When indicated, 3-D cell aggregates were exposed to other pro-inflammatory stimuli, i.e. *S. aureus* (MOI 10:1), lipopolysaccharide (LPS) (100 µg/mL) (Sigma-Aldrich), rhamnolipid (100 µg/mL) (Sigma-Aldrich) and H₂O₂ (1 mM), together with *R. mucilaginosa* for 4h. For longer term experiments, 3-D cell aggregates were exposed to 100 µg/mL LPS alone or in combination with *R. mucilaginosa* for 24h at an MOI of 1:1. For experiments with cell-free supernatant of *R. mucilaginosa*, cultures were centrifuged and filtered through a 0.22 µm PET filter membrane (GE Healthcare). To obtain lysed cell suspension, *R. mucilaginosa* cultures were subjected to a cold-heat cycle twice (i.e. 5 min ice followed by 5 min at 85 °C). Viability of lysed cells was checked by plating on nutrient agar, confirming no culturable bacteria. 3-D A549 cells were exposed for 4h to *P. aeruginosa* PAO1 (MOI 10:1) with or without *R. mucilaginosa* supernatant (100 µL cell-free supernatant and 150 µL GTSF-2 cell culture medium without FBS), lysed cells (100 µL lysed cell suspension initially containing 2.5 x 10⁶ cells which is equivalent to an MOI of 10:1, and 150 µL cell culture medium) or live cells as described earlier (MOI 10:1).

Cytotoxicity assays. After infection of the 3-D cells with various bacteria or exposure to other pro-inflammatory stimuli (LPS, rhamnolipid and H₂O₂), cell viability was assessed using the annexinV/PI (Life Technologies) and lactate dehydrogenase (LDH) (Sigma-Aldrich) assay, according to the manufacturer's instructions.

Bacterial cell adherence analysis. Bacterial adherence to the host cells was determined as described previously [43]. Previously developed selective media were used when host cells were co-exposed to *P. aeruginosa* and *R. mucilaginosa*, i.e. Luria Bertani (LB) agar supplemented with 1.25 mg/mL triclosan to select for *P. aeruginosa*, nutrient agar

supplemented with 5 mg/mL mupirocin and 10 mg/mL colistin sulphate to select for *R. mucilaginosa* [39].

Evaluation of IL-8 degradation. Recombinant IL-8 standard (Biolegend, San Diego, CA) at a concentration of 125 pg/mL was added to a *R. mucilaginosa* culture in GTSF-2 medium without serum (5×10^7 CFU/mL corresponding to an MOI 10:1) or to control medium. The IL-8 concentration was measured after 0, 15, 30, 60 and 90 min using an ELISA, as described below.

***In vivo* mouse model.** Twelve-week old female BALB/c ByJRj mice (Janvier Labs) were managed in accordance to the guidelines provided by the European Directive for Laboratory Animal Care (Directive 2010/63/EU of the European Parliament). The laboratory Animal Ethics Committee of the University of Antwerp authorized and approved all animal experiments in this study (file 2019-90). Intratracheal administration of *R. mucilaginosa* embedded in alginate beads in the presence or absence of LPS was done using a protocol described by Moser et al., 2009 [46], with adaptations described in the supplemental material. Embedding bacteria in alginate is a technique developed to retain a sufficient microbial load in the lungs over an extended time without immunosuppression [47]. In a preliminary experiment using *R. mucilaginosa* cell suspension for intratracheal administration, consistent colonization could not be obtained (supplemental material). Moreover, for *R. mucilaginosa*, the method used to prepare alginate beads removed bacterial clumps larger than 0.25 mm thereby limiting the risk of blocking the airways of the mice. Hence, embedding of *R. mucilaginosa* in alginate beads was used for all experiments. For preparation of the *R. mucilaginosa*-containing alginate beads, three independent cultures were pooled. Mice were instilled with 10 µg/50 µL LPS with or without *R. mucilaginosa* (either *R. mucilaginosa* DSM20746 or the CF isolate *R. mucilaginosa* B03V1S1C at the maximal dose that could be obtained in the alginate beads, i.e. $\sim 1 \times 10^5$ CFU mouse) embedded in alginate beads for 48 h. Mice were observed during this 48 h for fur quality, posture, state of activity, and respiratory symptoms and were weighted every 24 h. Mice were euthanized by

cervical dislocation 48 h post-infection. The left lung was homogenized and used for determination of the microbial load (by plate counting) as well as for cytokine quantification. The spleen and medial lobe of the liver were collected and homogenized to check for dissemination of the instilled bacteria (by plate counting). The right lung was collected in 1 mL of 4% PFA for histologic analysis. Sections for histological analysis were stained by H&E and were examined blindly and scored as previously described [48], using an EVOS FL Auto microscope (Life Technologies).

Quantification of *Rothia* sp. in respiratory samples. Archived, induced sputum samples were obtained from 85 adults with confirmed bronchiectasis and with a history of two or more infective exacerbations (associated with bacterial infection based on the requirement for supplemental systemic antibiotic therapy) in the preceding year, recruited as part of the BLESS randomized controlled trial [49]. Information on the patient cohort (incl. inclusion and exclusion criteria, sputum induction procedure) is provided in the Supplemental methods. The study was approved by the Mater Health Service human research ethics committee, and an informed consent for all participants was obtained. Induced sputum was collected at baseline, prior to any intervention and all patients had a sputum neutrophil abundance of $\geq 70\%$ (as a percentage of total sputum cells). All patients had a chronic lower airway infection. The relative abundance of *Rothia* sp. was measured in 79/85 samples using 16S rRNA gene amplicon sequencing, as described previously [50] and as detailed in the Supplemental methods. Sequence data are available at the NCBI Sequence Read Archive, accession number SRA128000. *R. mucilaginosa* absolute abundance was measured by quantitative PCR (qPCR) in 82/85 samples using the Qiagen Microbial DNA qPCR Assay for *R. mucilaginosa* (Catalog No. - BPID00297A). Gene copy numbers were determined by comparing to a standard curve as previously described [51].

Inflammatory marker quantification. For *in vitro* experiments, IL-8 secretion was measured in the cell culture supernatant by a Human IL-8 ELISA MAXTM Standard assay (Biolegend, San Diego, CA). For *in vivo* animal experiments, Macrophage Inflammatory

Protein (MIP)-2 secretion was measured in lung homogenate by a MIP-2 Mouse ELISA kit (LabNed, Amstelveen, NL). All other cytokines for *in vitro* cell culture and *in vivo* animal experiments were quantified by Bioplex Multiplex assays (Bio-Rad, Hercules, CA). Inflammatory markers were measured in the sputum of bronchiectasis patients using ELISA (BD Biosciences, San Jose, CA) for IL-8 and IL-1 β , and using Magnetic Luminex Performance Assay multiplex kits (R&D Systems, Minneapolis, MN) for matrix metalloproteinase (MMP)-1, MMP-8, and MMP-9, as described previously [52].

Quantitative reverse-transcription polymerase chain reaction (qRT-PCR)

array. 3-D A549 cells were infected with *P. aeruginosa* PAO1 or a combination of *P. aeruginosa* PAO1 and *R. mucilaginosa* DSM20746 as described above. After 4 h of infection, 3-D A549 cells were washed three times with HBSS and RNA protect reagent (Qiagen, Hilden, Germany) was added. Total cellular RNA was extracted using the Aurum Total RNA Mini Kit (Bio-Rad) and reverse transcribed into cDNA using the iScript advanced cDNA synthesis kit (Bio-Rad). The expression of various genes involved in inflammation was quantified using the Bacterial infections in normal airways PrimePCR panel (Bio-Rad) and SsoAdvanced SYBR Green supermix (Bio-Rad). qRT-PCR experiments were performed on a Bio-Rad CFX96 Real-Time System C1000 Thermal Cycler. TBP, GAPDH and HPRT1 were used as reference genes. Genes with an insufficient expression level were excluded from further analysis.

Analysis of NF- κ B activation. A 3-D epithelial cell model of NF- κ B-luciferase-transfected A549 cells (BPS Bioscience, San Diego, CA) was developed as described for the 3-D A549 model. Cells were exposed for 4 h to single or co-cultures of *P. aeruginosa* and *R. mucilaginosa* (or its cell-free supernatant) as described above. Likewise, a screening of NF- κ B activation by LPS (100 μ g/mL) with or without 36 isolates representing five different *Rothia* species (Table 1) was performed. When indicated, the effect of *Rothia* species (*R. mucilaginosa* DSM20146, *R. dentocariosa* HVOC18-02, *R. aeria* HVOC13-01 and *R. terrae* HVOC29-01) on NF- κ B pathway activation by LPS (100 μ g/mL) was evaluated under

microaerobic conditions (3% O₂, 5% CO₂, 92% N₂) in a BACTROX-2 Hypoxia chamber (SHEL LAB). The One-Step Luciferase Assay System (BPS Bioscience, San Diego, CA) was used to quantify NF-κB pathway activation, and luminescence was measured by an EnVision (Perkin Elmer) luminometer.

Western blot analysis. The Western blot experiments were done as previously [53]. Mouse monoclonal antibodies, at concentrations recommended by the manufacturer, were used to detect A20 (Santa Cruz Biotechnology, Inc), NFκB p65 (Santa Cruz Biotechnology, Inc) and p-IκB-α (Cell signaling) and a goat polyclonal antibody was used to detect IκB-α (Santa Cruz Biotechnology, Inc). As secondary antibody, an anti-mouse IgG HRP-linked Ab (Santa Cruz Biotechnology, Inc) or anti-goat IgG HRP-linked Ab (Santa Cruz Biotechnology, Inc) was used.

Statistical analysis. All *in vitro* experiments were carried out at least in biological triplicate. *In vitro* infection experiments contained two technical replicates for assessment of the viability, quantification of CFU by plating and quantification of cytokines. For animal experiments, MIP-2, CFU, disease symptoms in the animals, colonization and dissemination were determined for two independent experiments with *R. mucilaginosa* DSM20746. Validation of the *in vivo* data with another *R. mucilaginosa* strain (B03V1S1C), and quantification of additional cytokines as well as histological analysis were done for one experiment for both strains. Statistical analysis was performed using SPSS 24.0. The Shapiro-Wilk test was applied to evaluate normality of the data. For normally distributed data, differences between the means were assessed by an independent samples t-test or ANOVA followed by a Dunnett's post hoc analysis. Not normally distributed data were further analyzed by a Kruskal-Wallis non-parametric test or Mann-Whitney test. Statistical significance is assumed when p-values are <0.05. For correlation analysis, between *Rothia* species abundance (relative or absolute) and cytokine/matrix metalloproteinase concentrations, correlation coefficients and p values

were determined by either Pearson's test (r) for parametric distributions or Spearman's test (r_s) for non-parametric distributions.

RESULTS

***R. mucilaginosa* inhibits the production of pro-inflammatory cytokines by lung epithelial cells *in vitro*.**

Exposure of an *in vivo*-like 3-D alveolar epithelial model to *P. aeruginosa* PAO1 (MOI 30:1) induced high IL-8 production, while low or moderate IL-8 production was observed following exposure to *S. aureus* SP123, *S. anginosus* LMG14696, *A. xylosoxidans* LMG26680, *G. haemolysans* LMG18984 and *Rothia mucilaginosa* DSM20746 (Fig. 1A). When 3-D A549 cells were co-exposed to *P. aeruginosa* and one of each of the five other bacterial species, *R. mucilaginosa* completely abolished the *P. aeruginosa*-induced IL-8 response (Fig. 1B). *R. mucilaginosa* exposure also lowered the IL-8 response induced by *P. aeruginosa* at an MOI of 100:1 and 10:1 (Fig. S1A). The effect of *R. mucilaginosa* DSM20746 on *P. aeruginosa*-induced IL-8 production was confirmed with two other strains of *R. mucilaginosa* (ATCC49042; and a CF sputum isolate, B03V1S1C) (Fig. S1B). The three *R. mucilaginosa* strains also reduced the IL-8 response induced by various *P. aeruginosa* CF sputum isolates (Fig. S1B). Reduction in IL-8 response by *R. mucilaginosa* was confirmed using LPS (100 $\mu\text{g}/\text{mL}$) as the pro-inflammatory stimulus, both for short-term (4h) and long-term (24h) exposure (Fig. 1C). Under the experimental conditions tested, a similar number of *R. mucilaginosa* CFU was observed between the initial inoculum (0h) and the total CFU that associated with the host cells and were present in the surrounding liquid at 4h and 24h, indicating that bacteria remained viable throughout the experiment (Fig. S1C). After 4h, a slight increase in total *R. mucilaginosa* CFU was observed, compared to the inoculum (Fig. S1C).

R. mucilaginosa also significantly reduced IL-8 levels promoted by the Gram-positive pathogen *S. aureus* (MOI 10:1) in 3-D A549 cells (Fig. S1D). The anti-inflammatory effect of *R. mucilaginosa* was confirmed in a 3-D model of CF bronchial epithelial cells (IB-3 cell line) and in the CFTR corrected control (S9 cell line) (Fig. S1EF).

In addition, *R. mucilaginosa* reduced levels of other *P. aeruginosa*-induced pro-inflammatory cytokines (IL-6, IL-8, GM-CSF and MCP-1) (Fig. 1D). Exposure to *P. aeruginosa*, *R. mucilaginosa* or the combination showed normal morphology based on microscopic analysis, and cells retained more than 80% viability after infection (Fig. S2).

***R. mucilaginosa* lowers the LPS-induced pro-inflammatory response in an *in vivo* mouse model.**

Next, we evaluated the *in vivo* anti-inflammatory effect of *R. mucilaginosa* by measuring mouse lung inflammatory cytokine levels following LPS instillation, and LPS and *R. mucilaginosa* (either DSM20746 and B03V1S1C strains) co-exposure (Fig. 2A). After 48h of co-exposure, LPS-induced MIP-2 (homologue for human IL-8) was reduced by 40% by strain DSM20746 (Fig. 2B). The results obtained were validated using another *R. mucilaginosa* strain (B03V1S1C), which demonstrated a reduction of LPS-induced MIP-2 production of 70% (Fig. 2B). Levels of other cytokines (MCP-1, IL-6, IL-1 α , IL-5, IL-10, GM-CSF) were also significantly lower in mice exposed to LPS and *R. mucilaginosa* B03V1S1C compared to LPS alone (Fig. S3). The lungs of *R. mucilaginosa*-infected mice contained a similar number of CFU/mL bacteria in the presence and absence of LPS (Fig. 2C). No bacteria were detected in the liver and spleen suggesting no dissemination, and mice showed an overall normal fur quality, posture, body weight and no respiratory symptoms in all test conditions. H&E stained lung sections of LPS-instilled mice showed significantly more pronounced tissue damage compared to lung sections of mice co-exposed to LPS and *R. mucilaginosa* B03V1S1C, and the same trend for *R. mucilaginosa* DSM20746 was observed (Fig. 2D-E).

***Rothia* species inhibit NF- κ B activation in epithelial cells**

To decipher the mode of action of *R. mucilaginosa*, the expression of genes that are part of major pro-inflammatory pathways was evaluated in 3-D A549 cells exposed to *P. aeruginosa*, or *P. aeruginosa* and *R. mucilaginosa*. *R. mucilaginosa* co-exposure significantly downregulated the expression of genes encoding IL-8, IL-6 and pro-IL-1 β (Fig. 3) caused by *P. aeruginosa*. In addition, *R. mucilaginosa* significantly downregulated NFKB1 expression (Fig. 3). Regulation of NFKBIA, NFKBIE and REL genes showed a downward trend that further indicates an effect of *R. mucilaginosa* on the NF- κ B pathway.

The influence of *R. mucilaginosa* on activation of the NF- κ B pathway was confirmed in an NF- κ B-luciferase reporter 3-D A549 cell model, showing a significant reduction of NF- κ B activity by co-culturing *R. mucilaginosa* with *P. aeruginosa* compared to *P. aeruginosa* single exposure (Fig. 4A). The inhibition of the NF- κ B pathway by *R. mucilaginosa* was also shown using LPS as a pro-inflammatory stimulus and was observed for 36 isolates representing five different *Rothia* species from clinical and environmental sources (Fig. S4A-B). The anti-inflammatory effect of different *Rothia* species on NF- κ B pathway activation by LPS was also observed under microaerobic conditions (Fig. S4C), which can be encountered by microorganisms in the mucus of patients with chronic lung disease such as CF [54]. The minimal effective dose of *R. mucilaginosa* to inhibit *P. aeruginosa*-induced inflammation was an MOI of at least 5:1 for all doses of *P. aeruginosa* tested (up to MOI 100:1) (Fig. S5A). We also tested higher doses of *R. mucilaginosa* (MOI 100 and 1000) and the anti-inflammatory effect was confirmed (Fig. S5B).

We subsequently performed a Western blot analysis to investigate at which stage *R. mucilaginosa* affects NF- κ B signaling. After 4h co-culture of *P. aeruginosa* and *R. mucilaginosa*, *R. mucilaginosa* prevented *P. aeruginosa*-induced I κ B α phosphorylation (Fig. 4B-C). This suggests that *R. mucilaginosa* affects NF- κ B signaling upstream or at the level of the I κ B α kinase complex (IKK). In line with this, the expression of both I κ B α and A20, two NF- κ B target genes, was greatly reduced in the co-culture samples (Fig. 4C).

Finally, we excluded degradation of IL-8 or inhibition of *P. aeruginosa* adhesion to 3-D A549 epithelial cells by *R. mucilaginosa* as alternative explanations for the observed anti-inflammatory effect (Fig. S6).

***R. mucilaginosa* supernatant inhibits IL-8 production and NF- κ B pathway activation in response to pro-inflammatory stimuli in 3-D lung epithelial cells**

Exposure of 3-D A549 cells to *P. aeruginosa* PAO1 (MOI 10:1) in the presence of *R. mucilaginosa* cell-free supernatant, but not lysed cells, strongly reduced IL-8 production (Fig. 5A). We confirmed that *R. mucilaginosa* DSM20746 cell-free supernatant fully abolished LPS-stimulated NF- κ B pathway activation (Fig. 5B).

Inverse relationship between airway inflammation and *Rothia* spp. in patients with neutrophilic airways disease

Two culture-independent approaches were applied to measure *Rothia* spp. in induced sputum samples from patients with bronchiectasis, a neutrophilic airways disease. The first approach (measuring *R. mucilaginosa* absolute load) indicated that *R. mucilaginosa* load significantly inversely correlated with levels of IL-8 (Fig. 6A), and IL-1 β (Fig. 6B), as well as with those of metalloproteinases MMP-1 (Fig. 6C) and MMP-8 (Fig. 6D). There were no significant correlations between *R. mucilaginosa* and MMP-9 (Fig. 6E) or neutrophil % in sputum (Fig. 6F). In the second approach, we determined the relative abundance of *Rothia* and found it also inversely correlated with levels of IL-8, IL-1 β , MMP-1, and MMP-8. The correlation between *Rothia* relative abundance and MMP-9 was also significant. There was again no correlation between *Rothia* abundance and neutrophil % (Fig. S7).

Discussion

We report that common members of the lung microbiota belonging to the genus *Rothia* exert anti-inflammatory properties *in vitro*, and that for at least one (*R. mucilaginosa*) this effect is also apparent *in vivo*. Being frequently part of the oral microbiota and only rarely causing lung infection [55, 56], *R. mucilaginosa* is often considered part of salivary contamination of samples from the lower airways. However, comparison of the microbiome of the oral cavity with the lung microbiome suggests that *R. mucilaginosa* is not a contaminant [38, 57, 58]. The core lung microbiome varies inter-individually, yet *Rothia* sp. are detected in COPD and asthmatic patients, in pediatric and adult individuals with CF [23, 34, 36, 37, 59], and also in the lower airways of healthy people [60]. Nevertheless, little is known about its role in chronic lung disease [24, 61].

The presence of bacteria in the lower airways in chronic lung disease is conventionally considered as a contributor to the pathophysiology [13–15]. Results obtained in the present study strongly suggest that the presence of *R. mucilaginosa* in the airways is beneficial as it did not only inhibit the production of *P. aeruginosa*-induced pro-inflammatory cytokines, it also showed an inhibitory effect on the IL-8 response induced by LPS and by another important respiratory pathogen, *S. aureus*. The anti-inflammatory effect was confirmed for a large collection of *Rothia* species, and was also observed under microaerobic conditions. Since *Rothia* spp. are facultative anaerobes, it is likely that these microorganisms will colonize niches with low oxygen levels found in the lung mucus of patients with chronic lung disease [54]. Nevertheless, a minimal dose of *Rothia* was needed to obtain an anti-inflammatory effect *in vitro* for all doses of *P. aeruginosa* tested, suggesting a dose-dependent effect. The dose used most frequently throughout our study (MOI 10:1) is justified as a model for patients with chronic lung disease since a total bacterial MOI of ~100:1 has been reported for CF patients [62], and the relative abundance of *Rothia* varies between 1-40% [63, 64]. Also, in the BLESS cohort that was analyzed in our study, the mean relative abundance of *Rothia* was 9%, supporting the physiological relevance of the dose used.

Nevertheless, we cannot rule out that at some point, high loads of *Rothia* may result in a net pro-inflammatory effect in the lung environment, regardless of its anti-inflammatory properties. Very high doses of *R. mucilaginosa* (up to MOI of 1000) still exerted an anti-inflammatory effect *in vitro*; therefore, further research is needed to evaluate the load of *Rothia* that can be tolerated *in vivo*, without causing adverse effects.

R. mucilaginosa was also able to reduce the LPS-triggered production of pro-inflammatory cytokines in lung homogenates of mice, using an alginate bead model. The levels of several cytokines in mice exposed to empty alginate beads were similar to those of LPS-treated mice, which is in agreement with a previous study reporting inflammatory responses in mouse lungs after instillation with sterile alginate beads [65]. Nevertheless, *R. mucilaginosa* caused a clear decline in the inflammatory response of lung tissue regardless of the stimulus, and the degree of the anti-inflammatory effect was strain-dependent.

Interestingly, previous studies have shown a negative correlation between the relative abundance of *Rothia* spp. and sputum inflammatory markers, such as neutrophil elastase, IL-8 and IL-1 β in CF patients [66, 67]. A recent report found the relative abundance of the genus *Rothia* in expectorated sputum to be a positive predictor of lung function in patients with CF [68]. Not only were we able to confirm a negative correlation between *Rothia* spp. and inflammation for the BLESS cohort at the relative abundance level, but we also showed that absolute abundance of *R. mucilaginosa* was negatively correlated with inflammatory markers (based on IL-8 and IL-1 β levels) and mediators of airway remodeling (MMP-1 and MMP-8 levels). Levels of MMP-1, MMP-8, and MMP-9, which degrade extracellular matrix proteins [69], are increased in the airways of patients with neutrophilic airways disease, are inversely correlated with lung function [52], and contribute to irreversible airway damage [69]. We did not find an association between *Rothia* and neutrophil abundance. This is potentially attributable to relatively low levels of variation in neutrophil percentages between patients (all ≥ 70 %). Assessment of *Rothia* abundance in other cohorts of neutrophilic airways disease is

needed to confirm a possible anti-inflammatory effect of *Rothia* spp. in patients, and to determine the extent to which this might impair the progression of structural lung disease.

While several studies have associated an increased abundance of *Rothia* with positive health outcomes, it was recently demonstrated that the relative abundance of *Rothia* spp. was higher in a cohort of patients with a range of chronic lung diseases (severe asthma, COPD, bronchiectasis) [70] and in patients with tuberculosis as compared to healthy individuals [71]. It remains to be determined whether the increased *Rothia* relative abundance also implies an actual change in the absolute microbial load of that species, or merely reflects a decreased abundance of other (more dominant) species. Nevertheless, the study of Hong et al. indicated that *R. mucilaginosa* may serve as an anchor species for *M. tuberculosis* and 20 other taxa. It is possible that metabolic cross-feeding could alter the co-occurrence of other pathogenic or non-pathogenic species in the lung environment. For *R. mucilaginosa*, it was demonstrated that its metabolic products can cross-feed *P. aeruginosa* [72]. While we did not observe *R. mucilaginosa*-induced growth of *P. aeruginosa* in our study, long-term inter-species interactions are worth exploring further to evaluate whether commensal species such as *R. mucilaginosa* may influence overall community composition, in addition to exerting an anti-inflammatory activity. Furthermore, whether an altered *Rothia* abundance in the described and present studies is a driver of disease/disease markers or a consequence of an altered lung physiology (e.g. due to altered airway clearance or differential levels of reactive oxygen species, pro-inflammatory cytokines, mucins) remains a question to be fully addressed. The obtained data in animals suggests that supplementation of *Rothia* in the lungs may diminish the pro-inflammatory response to external stimuli, yet further exploration of the causal relation between *Rothia* abundance and inflammation in patients is needed.

The discovery of *Rothia* as an anti-inflammatory genus in the lung microbiota raises the question whether other non-pathogenic commensals in the respiratory tract, in particular originating from the oral cavity, may have immunomodulatory properties. Recent studies in animals [73] or *in vitro* [74] support this hypothesis. For example, pulmonary aspiration of

oral human commensals (*Prevotella melaninogenica*, *Veillonella parvula*, and *Streptococcus mitis*) in mice induces a T-helper cell type 17 (Th17) inflammatory phenotype that diminishes susceptibility to *Streptococcus pneumoniae*. Our data on cytokine production and on NF- κ B activation indicate that *R. mucilaginosa* prevents NF- κ B signaling, probably at the level of IKK activation. Indeed, IL-8, IL-1 β , IL-6, and TNF- α are regulated by NF- κ B through binding of pathogen-associated molecular patterns to TLRs³⁷. This is of particular interest since the NF- κ B pathway mediates the elevated innate immune response in patients with chronic lung diseases [75–84]. Cell-free supernatant exhibited anti-inflammatory activity, indicating that *R. mucilaginosa* secretes (an) anti-inflammatory mediator(s) that directly interferes with the NF- κ B pathway or induces host mediators that resolve inflammation. Since the anti-inflammatory activity was observed using both the pure TLR4 ligand LPS as well as different microbial species as the pro-inflammatory trigger, we can exclude that antimicrobial activity of *R. mucilaginosa* is causing the effect. Research to identify the immunomodulatory mediator(s) will be necessary to further understand how *Rothia* sp. modulate the pro-inflammatory response.

Understanding the contribution of potentially beneficial species to net inflammation could enable us to better understand variation in disease severity and progression between patients with chronic lung disease. Prospective studies to assess the clinical utility of *R. mucilaginosa* as a marker of airway inflammation, and the extent to which it may provide a basis for the development of novel therapeutic interventions, are now required.

Acknowledgements

We thank Catherine Greene for providing the CF cell lines, Matthew Parsek and Boo Tseng for providing *P. aeruginosa* CF127, and Joana Doci for help with the experiments. This work was funded by the Research Foundation Flanders (FWO). C.R is a recipient of an FWO-Strategic Basic Research (SB) fellowship (number 1S23117N). A.C. is a recipient of an FWO Odysseus grant (number G.0.E53.14N), and P.C., T.C. and A.C. received an FWO research grant (number G010119N). J.A. received funding from the European Union's Horizon 2020 research and innovation program under the Marie Skłodowska – Curie grant. (number 722467 Print-Aid consortium). G.R is supported by a Matthew Flinders Research Fellowship and a NHMRC Senior Research Fellowship. Y.D. is supported by a postdoctoral fellowship from the FWO (12T9118N).

Author contributions

A.C. conceptualized the study. A.C., C.R., T.C. are responsible for the overall study design. J.A., C.R., M.G. and L.O. performed the animal experiments. S.L.T. and S.S. performed DNA sequencing and qPCR experiments and data analysis. C.R. and L.O. performed the *in vitro* experiments and C.R. analyzed the data. L.B. and J.L.S. were responsible for clinical sampling. G.B.R., P.C., Y.D., M.S., L.V., A.B., C.C., H.V.A. and E.V. provided critical guidance in the experimental set-up, analysis and/or interpretation of results. C.R., A.W., M.M.T., G.B.R. and S.T. isolated bacterial strains used in this study. C.R., A.C., G.B.R., S.T. and J.A. wrote the manuscript. T.C., P.C., M.M.T., A.W., Y.D., L.V., C.C. revised the manuscript.

Declaration of Interests

A.C., C.R. and T.C. declare a patent application related to this work. All other authors declare no conflict of interest.

Table

Table 1. Overview of strains used in this study

Species	Strain designation	Source
<i>Pseudomonas aeruginosa</i>	PAO1 (ATCC 15692)	Wound
	AA2	Early CF isolate [85]
	AA44	Late CF isolate [85]
	AA43	Late CF isolate [85]
	CF127	CF isolate, hyper-biofilm former [86]
<i>Staphylococcus aureus</i>	SP123	Sputum of mechanically-ventilated patient [87]
<i>Streptococcus anginosus</i>	LMG14696	Human throat
<i>Achromobacter xylosoxidans</i>	LMG26680	Sputum of CF patient
<i>Gemella haemolysans</i>	LMG18984	Unknown
<i>Rothia mucilaginosa</i>	DSM20746	Throat
	ATCC49042	Bronchial secretion
	B03V1S1C	Sputum CF patient
	HVOC02-02	Oral cavity healthy volunteer
	HVOC02-03	Oral cavity healthy volunteer
	HVOC03-01	Oral cavity healthy volunteer
	HVOC03-02	Oral cavity healthy volunteer
	HVOC15-01	Oral cavity healthy volunteer
	HVOC23-01	Oral cavity healthy volunteer
	HVOC24-01	Oral cavity healthy volunteer
	PPP1	Sputum asthma patient
	PPIB2	Sputum asthma patient
	PPIA2	Sputum asthma patient
	PPR5A	Sputum asthma patient
	PPQ3	Sputum asthma patient
	PPW3A	Sputum asthma patient
	PPIB1	Sputum asthma patient
	PPL4C	Sputum asthma patient
	PPI6A	Sputum asthma patient

	PPL1A	Sputum asthma patient
	R-36507	Terrestrial microbial mat (Antarctica) [88]
<i>Rothia dentocariosa</i>	HVOC01-01	Oral cavity healthy volunteer
	HVOC05-01	Oral cavity healthy volunteer
	HVOC10-01	Oral cavity healthy volunteer
	HVOC18-02	Oral cavity healthy volunteer
	HVOC26-01	Oral cavity healthy volunteer
	HVOC27-01	Oral cavity healthy volunteer
	HVOC28-01	Oral cavity healthy volunteer
	PPS2A1	Sputum asthma patient
<i>Rothia terrae</i>	HVOC29-01	Oral cavity healthy volunteer
<i>Rothia amarae</i>	R-43211	Terrestrial microbial mat (Antarctica) [88]
	R-37581	Terrestrial microbial mat (Antarctica) [88]
	R-38387	Terrestrial microbial mat (Antarctica) [88]
	R-36663	Terrestrial microbial mat (Antarctica) [88]
<i>Rothia aeria</i>	HVOC04-01	Oral cavity healthy volunteer
	HVOC12-01	Oral cavity healthy volunteer
	HVOC13-01	Oral cavity healthy volunteer
	HVOC14-01	Oral cavity healthy volunteer

References

1. Tsirikla S, Dimakou K, Papaioannou A, Hillas G, Kostikas K, Loukides S, Papiris S, Koulouris N, Bakakos P. Non-invasive evaluation of airway inflammation in non-CF bronchiectasis. *10.1 Respir. Infect.* European Respiratory Society; 2016 [cited 2020 Jan 2]. p. PA2556.
2. Quinn TM, Hill AT. Non-cystic fibrosis bronchiectasis in the elderly: current perspectives. *Clin. Interv. Aging* Dove Press; 2018; 13: 1649–1656.
3. Dente FL, Bilotta M, Bartoli ML, Bacci E, Cianchetti S, Latorre M, Malagrino L, Nieri D, Roggi MA, Vagaggini B, Paggiaro P. Neutrophilic Bronchial Inflammation Correlates with Clinical and Functional Findings in Patients with Noncystic Fibrosis Bronchiectasis. *Mediators Inflamm.* Hindawi; 2015; 2015: 1–6.
4. Murdoch JR, Lloyd CM. Chronic inflammation and asthma. *Mutat. Res. Mol. Mech. Mutagen.* Elsevier; 2010; 690: 24–39.
5. Ishmael FT. The inflammatory response in the pathogenesis of asthma. *J. Am. Osteopath. Assoc.* 2011; 111: 11–17.
6. King PT. Inflammation in chronic obstructive pulmonary disease and its role in cardiovascular disease and lung cancer. *Clin Trans Med* 2015; 4: 26.
7. Rovina N, Koutsoukou A, Koulouris NG. Inflammation and Immune Response in COPD: Where Do We Stand? *Mediators Inflamm.* Hindawi Publishing Corporation; 2013; 2013.
8. Dhooghe B, Noël S, Huaux F, Leal T. Lung inflammation in cystic fibrosis: Pathogenesis and novel therapies ☆. *Clin. Biochem.* 2013; 2014: 8.
9. Cantin AM, Hartl D, Konstan MW, Chmiel JF. Inflammation in cystic fibrosis lung disease: Pathogenesis and therapy. *J. Cyst. Fibros.* Elsevier; 2015; 14: 419–430.

10. Ind PW. COPD disease progression and airway inflammation: uncoupled by smoking cessation. *Eur. Respir. J.* European Respiratory Society; 2005; 26: 764–766.
11. Simmons MS, Connett JE, Nides MA, Lindgren PG, Kleerup EC, Murray RP, Bjornson WM, Tashkin DP. Smoking reduction and the rate of decline in FEV1: results from the Lung Health Study. *Eur. Respir. J.* 2005; 25: 1011–1017.
12. Venkataraman A, Bassis CM, Beck JM, Young VB, Curtis JL, Huffnagle GB, Schmidt TM. Application of a Neutral Community Model To Assess Structuring of the Human Lung Microbiome. *MBio* 2015; 6.
13. Budden KF, Shukla SD, Rehman SF, Bowerman KL, Keely S, Hugenholtz P, Armstrong-James DPH, Adcock IM, Chotirmall SH, Chung KF, Hansbro PM. Functional effects of the microbiota in chronic respiratory disease. *Lancet Respir. Med.* Elsevier Ltd; 2019; 2600: 1–14.
14. Earl CS, An S, Ryan RP. The changing face of asthma and its relation with microbes. *Trends Microbiol.* Elsevier; 2015; 23: 408–418.
15. Cope EK. Host-Microbe Interactions in Airway Disease: toward Disease Mechanisms and Novel Therapeutic Strategies. *mSystems* 2018; 3.
16. Filkins LM, O 'toole GA. Cystic Fibrosis Lung Infections: Polymicrobial, Complex, and Hard to Treat. *PLOS Pathog.* 2015; 11: e1005258.
17. Filkins LM, Graber JA, Olson DG, Dolben EL, Lynd LR, Bhujju S, O'Toole GA. Coculture of *Staphylococcus aureus* with *Pseudomonas aeruginosa* Drives *S. aureus* towards Fermentative Metabolism and Reduced Viability in a Cystic Fibrosis Model. DiRita VJ, editor. *J. Bacteriol.* 2015; 197: 2252–2264.
18. Rada B. Interactions between Neutrophils and *Pseudomonas aeruginosa* in Cystic Fibrosis. *Pathogens* 2017; 6: 10.

19. Martínez-García MA, Soler-Cataluña JJ, Perpiñá-Tordera M, Román-Sánchez P, Soriano J. Factors associated with lung function decline in adult patients with stable non-cystic fibrosis bronchiectasis. *Chest* 2007; 132: 1565–1572.
20. Yang X, Li H, Ma Q, Zhang Q, Wang C. Neutrophilic Asthma Is Associated with Increased Airway Bacterial Burden and Disordered Community Composition. *Biomed Res. Int. Hindawi*; 2018; 2018.
21. Beasley V, Joshi P V., Singanayagam A, Molyneaux PL, Johnston SL, Mallia P. Lung microbiology and exacerbations in COPD. *Int. J. COPD* 2012; 7: 555–569.
22. Huffnagle GB, Dickson RP. The Bacterial Microbiota in Inflammatory Lung Diseases. *Clin Immunol.* 2015; 159: 177–182.
23. Coburn B, Wang PW, Diaz Caballero J, Clark ST, Brahma V, Donaldson S, Zhang Y, Surendra A, Gong Y, Elizabeth Tullis D, Yau YCW, Waters VJ, Hwang DM, Guttman DS. Lung microbiota across age and disease stage in cystic fibrosis. *Sci. Rep.* 2015; 5.
24. Tunney MM, Field TR, Moriarty TF, Patrick S, Doering G, Muhlebach MS, Wolfgang MC, Boucher R, Gilpin DF, McDowell A, Elborn JS. Detection of anaerobic bacteria in high numbers in sputum from patients with cystic fibrosis. *Am. J. Respir. Crit. Care Med.* 2008; 177: 995–1001.
25. Dickson RP, Huffnagle GB. The Lung Microbiome: New Principles for Respiratory Bacteriology in Health and Disease. *PLOS Pathog.* 2015; 11.
26. Moffatt MF, Cookson WO. The lung microbiome in health and disease. *Clin. Med. (Northfield. Il).* 2017; 17: 525–529.

27. Huang YJ, Charlson ES, Collman RG, Colombini-Hatch S, Martinez FD, Senior RM. The role of the lung microbiome in health and disease. A National Heart, Lung, and Blood Institute workshop report. *Am. J. Respir. Crit. Care Med.* American Thoracic Society; 2013; 187: 1382–1387.
28. Lobionda S, Sittipo P, Kwon Y, Lee YK. The Role of Gut Microbiota in Intestinal Inflammation with Respect to Diet and Extrinsic Stressors. *Microorganisms* 2019; Aug: 271.
29. Viennois E, Gewirtz AT, Chassaing B. Chronic Inflammatory Diseases: Are We Ready for Microbiota-based Dietary Intervention? *Cell. Mol. Gastroenterol. Hepatol.* Elsevier; 2019; 8: 61–71.
30. Ferreira CM, Vieira AT, Vinolo MAR, Oliveira FA, Curi R, Martins FDS. The Central Role of the Gut Microbiota in Chronic Inflammatory Diseases. *J. Immunol. Res.* 2014; 2014.
31. Zhao J, Schloss PD, Kalikin LM, Carmody LA, Foster BK, Petrosino JF, Cavalcoli JD, VanDevanter DR, Murray S, Li JZ, Young VB, LiPuma JJ. Decade-long bacterial community dynamics in cystic fibrosis airways. *Proc. Natl. Acad. Sci. U. S. A.* 2012; 109: 5809–5814.
32. Coburn B, Wang PW, Diaz Caballero J, Clark ST, Brahma V, Donaldson S, Zhang Y, Surendra A, Gong Y, Elizabeth Tullis D, Yau YCW, Waters VJ, Hwang DM, Guttman DS. Lung microbiota across age and disease stage in cystic fibrosis. *Sci. Rep.* 2015; 5.
33. Surette MG. The cystic fibrosis lung microbiome. *Ann. Am. Thorac. Soc.* 2014; 11 Suppl 1: S61-5.

34. Arrieta M-C, Stiemsma LT, Dimitriu PA, Thorson L, Russell S, Yurist-Doutsch S, Kuzeljevic B, Gold MJ, Britton HM, Lefebvre DL, Subbarao P, Mandhane P, Becker A, McNagny KM, Sears MR, Kollmann T, CHILD Study Investigators the CS, Mohn WW, Turvey SE, et al. Early infancy microbial and metabolic alterations affect risk of childhood asthma. *Sci. Transl. Med.* American Association for the Advancement of Science; 2015; 7: 307ra152.
35. Muhlebach MS, Zorn BT, Esther CR, Hatch JE, Murray CP, Turkovic L, Ranganathan SC, Boucher RC, Stick SM, Wolfgang MC. Initial acquisition and succession of the cystic fibrosis lung microbiome is associated with disease progression in infants and preschool children. Parsek MR, editor. *PLoS Pathog.* Public Library of Science; 2018; 14: e1006798.
36. Sokolowska M, Frei R, Lunjani N, Akdis CA, O'Mahony L. Microbiome and asthma. *Asthma Res. Pract.* BioMed Central; 2018; 4: 1.
37. Wang Z, Bafadhel M, Haldar K, Spivak A, Mayhew D, Miller BE, Tal-Singer R, Johnston SL, Ramsheh MY, Barer MR, Brightling CE, Brown JR. Lung microbiome dynamics in COPD exacerbations. *Eur Respir J* 2016; 47: 1082–1092.
38. Lim YW, Schmieder R, Haynes M, Furlan M, Matthews TD, Whiteson K, Poole SJ, Hayes CS, Low DA, Maughan H, Edwards R, Conrad D, Rohwer F. Mechanistic Model of *Rothia mucilaginosa* Adaptation toward Persistence in the CF Lung, Based on a Genome Reconstructed from Metagenomic Data. Kreindler JL, editor. *PLoS One* Public Library of Science; 2013; 8: e64285.
39. Vandeplassche E, Coenye T, Crabbé A. Developing selective media for quantification of multispecies biofilms following antibiotic treatment. *PLoS One* 2017; 12: 1–15.
40. Vandeplassche E, Sass A, Lemarcq A, Dandekar AA, Coenye T, Crabbé A. In vitro evolution of *Pseudomonas aeruginosa* AA2 biofilms in the presence of cystic fibrosis lung microbiome members. *Sci. Rep.* 2019; 9: 1–14.

41. Barrila J, Radtke AL, Crabbé A, Sarker SF, Herbst-Kralovetz MM, Ott CM, Nickerson CA. Organotypic 3D cell culture models: using the rotating wall vessel to study host–pathogen interactions. *Nat. Rev. Microbiol.* Nature Publishing Group; 2010; 8: 791–801.
42. Carterson AJ, Bentrup KH, Ott CM, Clarke MS, Pierson DL, Vanderburg CR, Buchanan KL, Nickerson CA, Schurr MJ. A549 Lung Epithelial Cells Grown as Three-Dimensional Aggregates: Alternative Tissue Culture Model for *Pseudomonas aeruginosa* Pathogenesis A549 Lung Epithelial Cells Grown as Three-Dimensional Aggregates: Alternative Tissue Culture Model for *Pseudomonas*. *Infect. Immun.* 2005; 73: 1129–1140.
43. Crabbé A, Liu Y, Matthijs N, Rigole P, De C, Fuente-Núñez L, Davis R, Ledesma MA, Sarker S, Houdt R Van, Hancock REW, Coenye T, Nickerson CA, De La Fuente-Núñez C, Davis R, Ledesma MA, Sarker S, Van Houdt R, Hancock REW, et al. Antimicrobial efficacy against *Pseudomonas aeruginosa* biofilm formation in a three-dimensional lung epithelial model and the influence of fetal bovine serum. *Nat. Publ. Gr.* Nature Publishing Group; 2017; 7: 43321.
44. Crabbé A, Sarker SF, Houdt R Van, Ott CM, Leys N, Cornelis P, Nickerson CA. Alveolar epithelium protects macrophages from quorum sensing-induced cytotoxicity in a three-dimensional co-culture model. *Cell. Microbiol.* 2011; 13: 469–481.
45. Gruenert DC, Willems M, Cassiman JJ, Frizzell RA. Established cell lines used in cystic fibrosis research. *J. Cyst. Fibros.* 2004; 3: 191–196.
46. Moser C, Van Gennip M, Bjarnsholt T, Jensen PØ, Lee B, Hougen HP, Calum H, Ciofu O, Givskov M, Molin SØ, HØiby N. Novel experimental *Pseudomonas aeruginosa* lung infection model mimicking long-term host-pathogen interactions in cystic fibrosis. *Apmis* 2009; 117: 95–107.

47. Sønderholm M, Kragh KN, Koren K, Jakobsen TH, Darch SE, Alhede M, Jensen PØ, Whiteley M, Kühl M, Bjarnsholt T. Pseudomonas aeruginosa Aggregate Formation in an Alginate Bead Model System Exhibits In Vivo-Like Characteristics. *Appl. Environ. Microbiol.* American Society for Microbiology; 2017; 83.
48. Cigana C, Lorè NI, Riva C, De Fino I, Spagnuolo L, Sipione B, Rossi G, Nonis A, Cabrini G, Bragonzi A. Tracking the immunopathological response to Pseudomonas aeruginosa during respiratory infections. *Sci. Rep.* 2016; 6.
49. Serisier DJ, Martin ML, McGuckin MA, Chen AC, Brain B, Biga S, Schlebusch S, Dash P, Bowler S. Effect of Long-term, Low-Dose Erythromycin on Pulmonary Exacerbations Among Patients With Non – Cystic Fibrosis Bronchiectasis. *Jama* 2013; 309: 1260–1267.
50. Rogers GB, Zain NMM, Bruce KD, Burr LD, Chen AC, Rivett DW, McGuckin MA, Serisier DJ. A novel microbiota stratification system predicts future exacerbations in bronchiectasis. *Ann. Am. Thorac. Soc.* 2014; 11: 496–503.
51. Taylor SL, Leong LEX, Mobegi FM, Choo JM, Wesselingh S, Yang IA, Upham JW, Reynolds PN, Hodge S, James AL, Jenkins C, Peters MJ, Baraket M, Marks GB, Gibson PG, Rogers GB, Simpson JL. Long-Term Azithromycin Reduces Haemophilus influenzae and Increases Antibiotic Resistance in Severe Asthma. *Am. J. Respir. Crit. Care Med.* 2019; 200: 309–317.
52. Taylor SL, Rogers GB, Chen ACH, Burr LD, McGuckin MA, Serisier DJ. Matrix metalloproteinases vary with airway microbiota composition and lung function in non-cystic fibrosis bronchiectasis. *Ann. Am. Thorac. Soc.* 2015; 12: 701–707.
53. Takahashi N, Vereecke L, Bertrand MJM, Duprez L, Berger SB, Divert T, Gonçalves A, Sze M, Gilbert B, Kourula S, Goossens V, Lefebvre S, Günther C, Becker C, Bertin J, Gough PJ, Declercq W, van Loo G, Vandenabeele P. RIPK1 ensures intestinal homeostasis by protecting the epithelium against apoptosis. *Nature* 2014; 513: 95–99.

54. Worlitzsch D, Tarran R, Ulrich M, Schwab U, Cekici A, Meyer KC, Birrer P, Bellon G, Berger J, Weiss T, Botzenhart K, Yankaskas JR, Randell S, Boucher RC, Döring G. Effects of reduced mucus oxygen concentration in airway Pseudomonas infections of cystic fibrosis patients. *J. Clin. Invest.* 2002; 109: 317–325.
55. Willner S, Imam Z, Hader I. Rothia dentocariosa Endocarditis in an Unsuspecting Host: A Case Report and Literature Review [Internet]. *Case Reports Cardiol.* 2019.
56. Maraki S, Papadakis IS. *Rothia mucilaginosa* pneumonia: a literature review. *Infect. Dis. (Auckl).* 2015; 47: 125–129.
57. Sverrild A, Kiilerich P, Brejnrod A, Pedersen R, Porsbjerg C, Bergqvist A, Erjefält JS, Kristiansen K, Backer V. Eosinophilic airway inflammation in asthmatic patients is associated with an altered airway microbiome. *J. Allergy Clin. Immunol.* 2017; 140: 407-417.e11.
58. Tsuzukibashi O, Uchibori S, Kobayashi T, Umezawa K, Mashimo C, Nambu T, Saito M, Hashizume-Takizawa T, Ochiai T. Isolation and identification methods of Rothia species in oral cavities. *J. Microbiol. Methods* Elsevier B.V.; 2017; 134: 21–26.
59. Muhlebach MS, Hatch JE, Einarsson GG, Mcgrath SJ, Gilipin DF, Lavelle G, Mirkovic B, Murray MA, McNally P, Gotman N, Thomas SD, Wolfgang MC, Gilligan PH, Mcelvaney NGJ, Elborn S, Boucher RC, Tunney MM. Anaerobic bacteria cultured from CF airways correlate to milder disease-a multisite study. *Eur Respir J* 2018; 52: 1800242.
60. Einarsson GG, Comer DM, McIlreavey L, Parkhill J, Ennis M, Tunney MM, Elborn JS. Community dynamics and the lower airway microbiota in stable chronic obstructive pulmonary disease, smokers and healthy non-smokers. *Thorax* 2016; 71: 795–803.

61. Laguna TA, Wagner BD, Williams CB, Stevens MJ, Robertson CE, Welchlin CW, Moen CE, Zemanick ET, Harris JK. Airway Microbiota in Bronchoalveolar Lavage Fluid from Clinically Well Infants with Cystic Fibrosis. Wilson BA, editor. *PLoS One* Blackwell Publishing Company; 2016; 11: e0167649.
62. Sze MA, Dimitriu PA, Hayashi S, Elliott WM, McDonough JE, Gosselink J V., Cooper J, Sin DD, Mohn WW, Hogge JC. The lung tissue microbiome in chronic obstructive pulmonary disease. *Am. J. Respir. Crit. Care Med.* 2012; 185: 1073–1080.
63. Cuthbertson L, Walker AW, Oliver AE, Rogers GB, Rivett DW, Hampton TH, Ashare A, Elborn JS, De Soyza A, Carroll MP, Hoffman LR, Lanyon C, Moskowitz SM, O'Toole GA, Parkhill J, Planet PJ, Teneback CC, Tunney MM, Zuckerman JB, et al. Lung function and microbiota diversity in cystic fibrosis. *Microbiome* Microbiome; 2020; 8: 1–13.
64. Frayman KB, Armstrong DS, Carzino R, Ferkol TW, Grimwood K, Storch GA, Teo SM, Wylie KM, Ranganathan SC. The lower airway microbiota in early cystic fibrosis lung disease: a longitudinal analysis. *Thorax* 2017; 72: 1104–1112.
65. Bielen K, 's Jongers B, Malhotra-Kumar S, Jorens PG, Goossens H, Kumar-Singh S. Animal models of hospital-acquired pneumonia: current practices and future perspectives. *Ann. Transl. Med.* AME Publications; 2017; 5: 132.
66. Zemanick ET, Wagner BD, Robertson CE, Stevens MJ, Szeffler SJ, Accurso FJ, Sagel SD, Harris JK. Assessment of airway microbiota and inflammation in cystic fibrosis using multiple sampling methods. *Ann. Am. Thorac. Soc.* American Thoracic Society; 2015; 12: 221–229.
67. Zemanick ET, Harris JK, Wagner BD, Robertson CE, Sagel SD, Stevens MJ, Accurso FJ, Laguna TA. Inflammation and airway microbiota during cystic fibrosis pulmonary exacerbations. *PLoS One* Public Library of Science; 2013; 8: e62917.

68. Zhao CY, Hao Y, Wang Y, Varga JJ, Stecenko AA, Goldberg JB, Brown SP. Microbiome data enhances predictive models of lung function in people with cystic fibrosis. *J. Infect. Dis.* 2020; .
69. Vandembroucke RE, Dejonckheere E, Libert C. Series “Matrix metalloproteinases in lung health and disease”: A therapeutic role for matrix metalloproteinase inhibitors in lung diseases? *Eur. Respir. J.* 2011; 38: 1200–1214.
70. Aogáin M Mac, Lau KJX, Cai Z, Narayana JK, Purbojati RW, Drautz-Moses DI, Gaultier NE, Jaggi TK, Tiew PY, Ong TH, Koh MS, Hou ALY, Abisheganaden JA, Tsaneva-Atanasova K, Schuster SC, Chotirmall SH. Metagenomics reveals a core macrolide resistome related to microbiota in chronic respiratory disease. *Am. J. Respir. Crit. Care Med.* 2020; 202: 433–447.
71. Hong B young, Paulson JN, Stine OC, Weinstock GM, Cervantes JL. Meta-analysis of the lung microbiota in pulmonary tuberculosis. *Tuberculosis Elsevier*; 2018; 109: 102–108.
72. Gao B, Gallagher T, Zhang Y, Elbadawi-Sidhu M, Lai Z, Fiehn O, Whiteson KL. Tracking Polymicrobial Metabolism in Cystic Fibrosis Airways: *Pseudomonas aeruginosa* Metabolism and Physiology Are Influenced by *Rothia mucilaginosa*-Derived Metabolites. .
73. Wu BG, Sulaiman I, Tsay JCJ, Perez L, Franca B, Li Y, Wang J, Gonzalez AN, El-Ashmawy M, Carpenito J, Olsen E, Sauthoff M, Yie K, Liu X, Shen N, Clemente JC, Kapoor B, Zangari T, Mezzano V, et al. Episodic aspiration with oral commensals induces a MyD88-dependent, pulmonary T-helper cell type 17 response that mitigates susceptibility to streptococcus pneumoniae. *Am. J. Respir. Crit. Care Med.* 2021; 203: 1099–1111.

74. Dickson RP, Erb-Downward JR, Falkowski NR, Hunter EM, Ashley SL, Huffnagle GB. The lung microbiota of healthy mice are highly variable, cluster by environment, and reflect variation in baseline lung innate immunity. *Am. J. Respir. Crit. Care Med.* 2018; 198: 497–508.
75. Bodas M, Vij N. The NF-kappaB signaling in cystic fibrosis lung disease: pathophysiology and therapeutic potential. *Discov. Med.* 2010; 9: 346–356.
76. Alvira CM. Nuclear factor-kappa-B signaling in lung development and disease: One pathway, numerous functions. *Birth Defects Res. Part A - Clin. Mol. Teratol.* 2014; 100: 202–216.
77. Jacquot J, Tabary O, Le Rouzic P, Clement A. Airway epithelial cell inflammatory signalling in cystic fibrosis. *Int. J. Biochem. Cell Biol.* 2008; 40: 1703–1715.
78. Chung K. Cytokines as Targets in Chronic Obstructive Pulmonary Disease. *Curr. Drug Targets* 2006; 7: 675–681.
79. Schuliga M. NF-kappaB Signaling in Chronic Inflammatory Airway Disease. *Biomolecules* 2015; 5: 1266–1283.
80. Barnes PJ, Adcock IM. NF-kB: a pivotal role in asthma and a new target for therapy. *TiPS* Raven Press 3 Fredholm; 1997; 18: 46–50.
81. Hart LA, Krishnan VL, Adcock IM, Barnes PJ, Chung KF. Activation and Localization of Transcription Factor, Nuclear Factor-B, in Asthma. *Am J Respir Crit Care Med* 1998; 158: 1585–1592.
82. Gagliardo R, Chanez P, Mathieu M, Bruno A, Costanzo G, Gougat C, Vachier I, Bousquet J, Bonsignore G, Vignola AM. Persistent Activation of Nuclear Factor-B Signaling Pathway in Severe Uncontrolled Asthma. *Am J Respir Crit Care Med* 2003; 168: 1190–1198.

83. Pantano C, Ather JL, Alcorn JF, Poynter ME, Brown AL, Guala AS, Beuschel SL, Allen GB, Whittaker LA, Bevelander M, Irvin CG, Janssen-Heininger YMW. Nuclear Factor- κ B Activation in Airway Epithelium Induces Inflammation and Hyperresponsiveness. *Am J Respir Crit Care Med* 2008; 177: 959–969.
84. Belchamber KBR, Donnelly LE. Pharmacology & Therapeutics Targeting defective pulmonary innate immunity – A new therapeutic option? *Pharmacol. Ther.* Elsevier Inc.; 2020; 209: 107500.
85. De Soyza A, Hall AJ, Mahenthiralingam E, Drevinek P, Kaca W, Drulis-Kawa Z, Stoitsova SR, Toth V, Coenye T, Zlosnik JEA, Burns JL, Sá-Correia I, De Vos D, Pirnay J-P, Kidd TJ, Reid D, Manos J, Klockgether J, Wiehlmann L, et al. Developing an international *Pseudomonas aeruginosa* reference panel on behalf of EU FP7 funded COST Action BM1003 " Cell surface virulence determinants of cystic fibrosis pathogens " *Microbiologyopen* 2013; 2: 1010–1023.
86. Colvin KM, Irie Y, Tart CS, Urbano R, Whitney JC, Ryder C, Howell PL, Wozniak DJ, Parsek MR. The Pel and Psl polysaccharides provide *Pseudomonas aeruginosa* structural redundancy within the biofilm matrix. *Environ. Microbiol.* 2012; 14: 1913–1928.
87. Vandecandelaere I, Matthijs N, Van Nieuwerburgh F, Deforce D, Vosters P, De Bus L, Nelis HJ, Depuydt P, Coenye T, Depuydt P, Myny D, Blot S, Augustyn B, Heo S, Haase E, Lesse A, Gill S, Scannapieco F, Adair C, et al. Assessment of Microbial Diversity in Biofilms Recovered from Endotracheal Tubes Using Culture Dependent and Independent Approaches. Highlander SK, editor. *PLoS One* Public Library of Science; 2012; 7: e38401.
88. Peeters K, Verleyen E, Hodgson DA, Convey P, Ertz D, Vyverman W, Willems A. Heterotrophic bacterial diversity in aquatic microbial mat communities from Antarctica. *Polar Biol.* 2012; 35: 543–554.

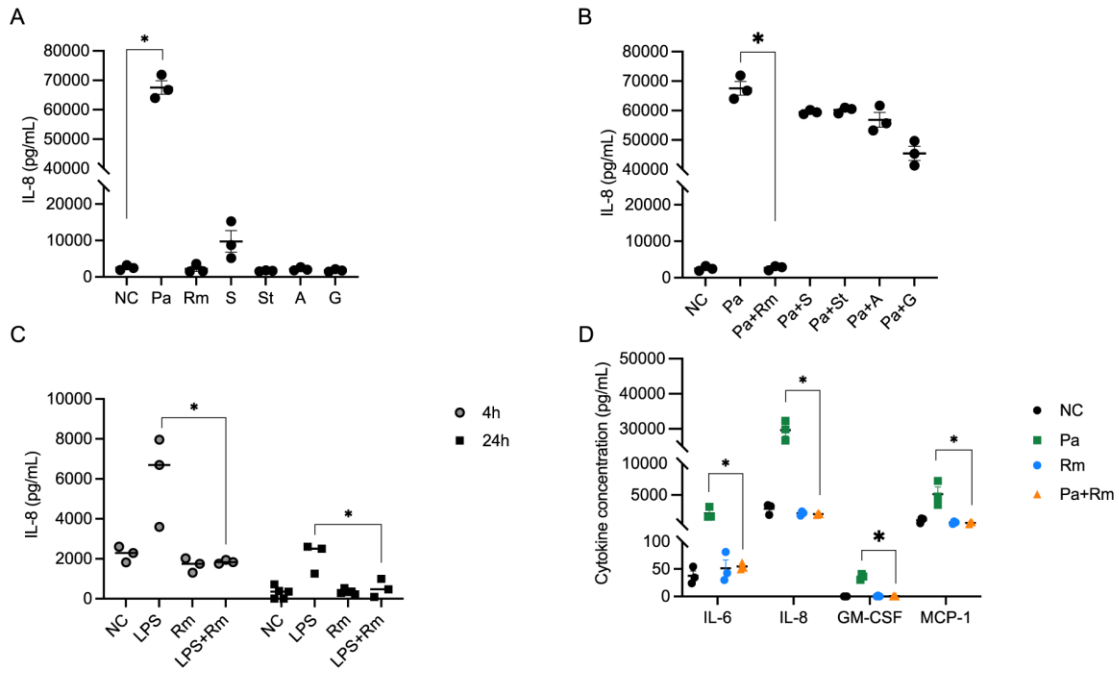


Figure 1. 3-D lung epithelial responses to pro-inflammatory stimuli in the presence and absence of members of the lung microbiota. (A) IL-8 production by 3-D A549 cells after 4h exposure to single bacterial cultures or (B) to co-cultures of various lung microbiota members with *P. aeruginosa* PAO1 at MOI 30:1. (C) IL-8 production by 3-D A549 cells after 4h or 24h exposure to 100 µg/mL LPS alone or in co-culture with *R. mucilaginosa* at an MOI 10:1 (4h) or 1:1 (24h). (D) IL-6, IL-8, GM-CSF and MCP-1 production of 3-D A549 cells after 4 h exposure to *P. aeruginosa* alone or in co-culture with *R. mucilaginosa* at MOI 10:1. Data represent the mean IL-8 concentration (pg/mL) (A,B,D) or mean log cytokine concentration (pg/mL) ± SEM (C), n ≥ 3, * p<0.05, ** p<0.001. NC= negative control, uninfected 3-D epithelial cells in serum-free medium; Pa = *P. aeruginosa* PAO1; S= *S. aureus* SP123; St= *S. anginosus* LMG 14696; A= *A. xylosoxidans* LMG 26680; G= *G. haemolysans* LMG 18984; Rm = *R. mucilaginosa* DSM20746

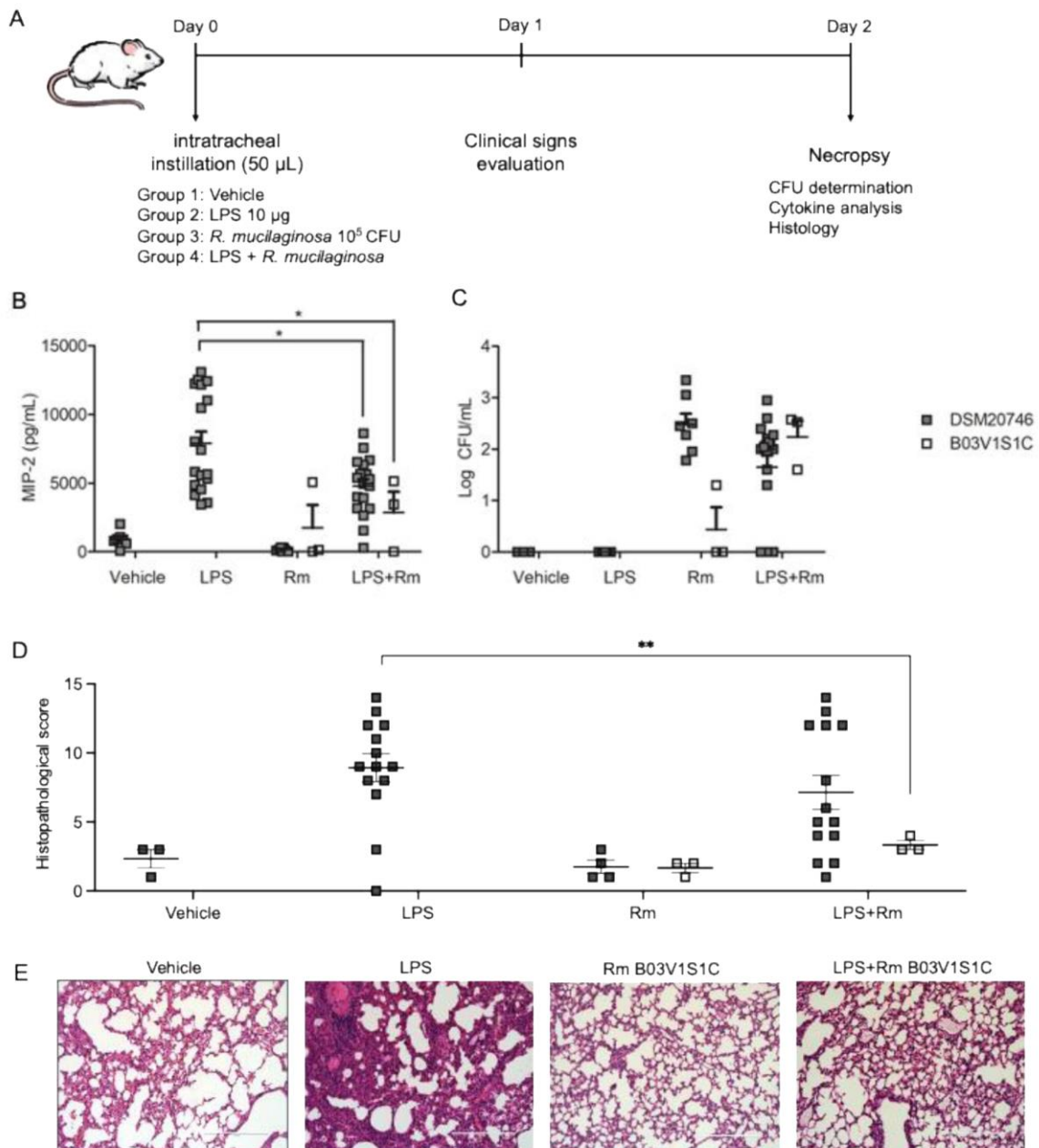


Figure 2. Influence of *R. mucilaginosa* on the *in vivo* responses to LPS. (A) Time-line animal infection and necropsy (B) MIP-2 concentration (measured by ELISA) and (C) number of CFU/mL in mice lung homogenates after 48 h exposure to sterile beads (vehicle) (n=7), LPS (n=18), *R. mucilaginosa* suspension (n=9 for *R. mucilaginosa* DSM20746 and n=3 for *R. mucilaginosa* B03V1S1C) or a combination of LPS and *R. mucilaginosa* (n=18 for *R. mucilaginosa* DSM20746 and n=3 for *R. mucilaginosa* B03V1S1C). (D) Lung histopathological score on H&E stained sections of the right lung. (E) Lung H&E stained

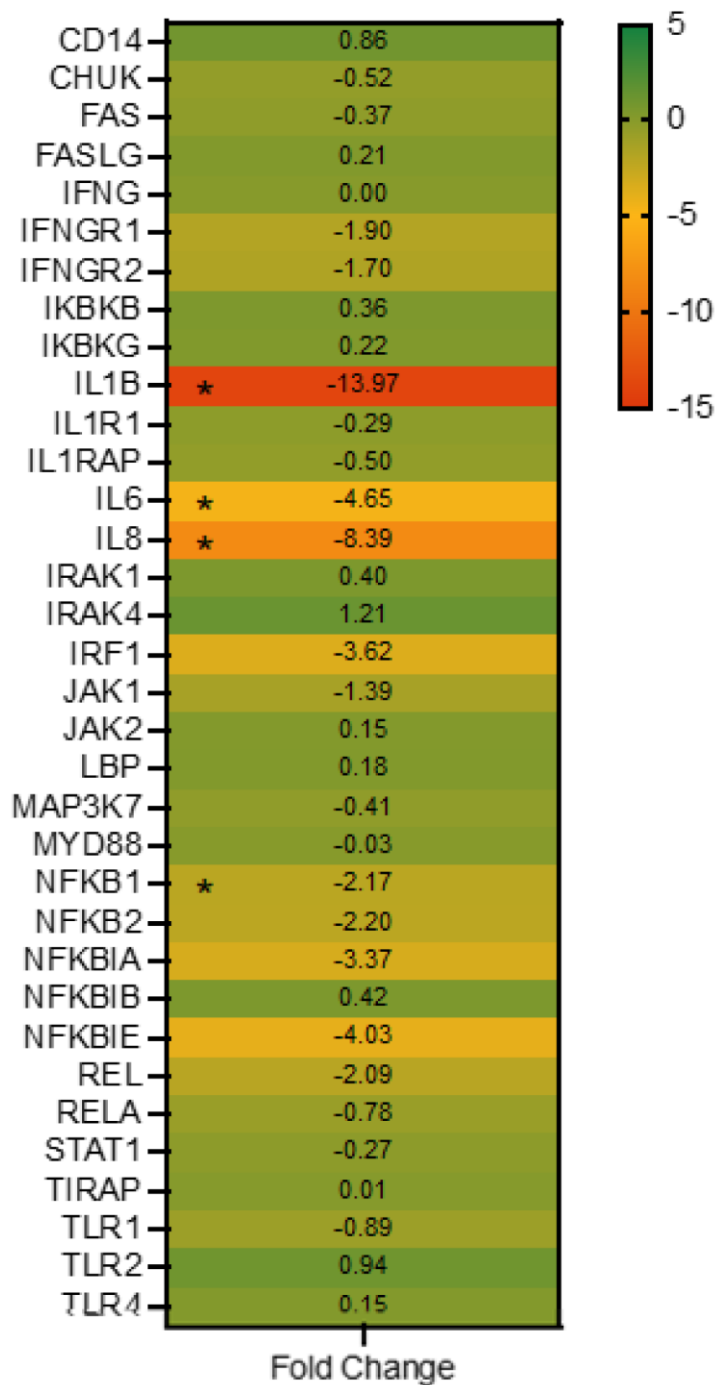


Figure 3. Differential expression of genes involved in inflammation by 3-D A549 alveolar epithelial cells exposed to *P. aeruginosa* versus *P. aeruginosa* in combination with *R. mucilaginosa*. Quantitative RT-PCR analysis, showing average fold changes in mRNA levels of 3-D A549 cells stimulated by *P. aeruginosa* PAO1 versus a co-culture of *P. aeruginosa* and *R. mucilaginosa*. n = 3, * statistically significant (p < 0.05) fold-change.

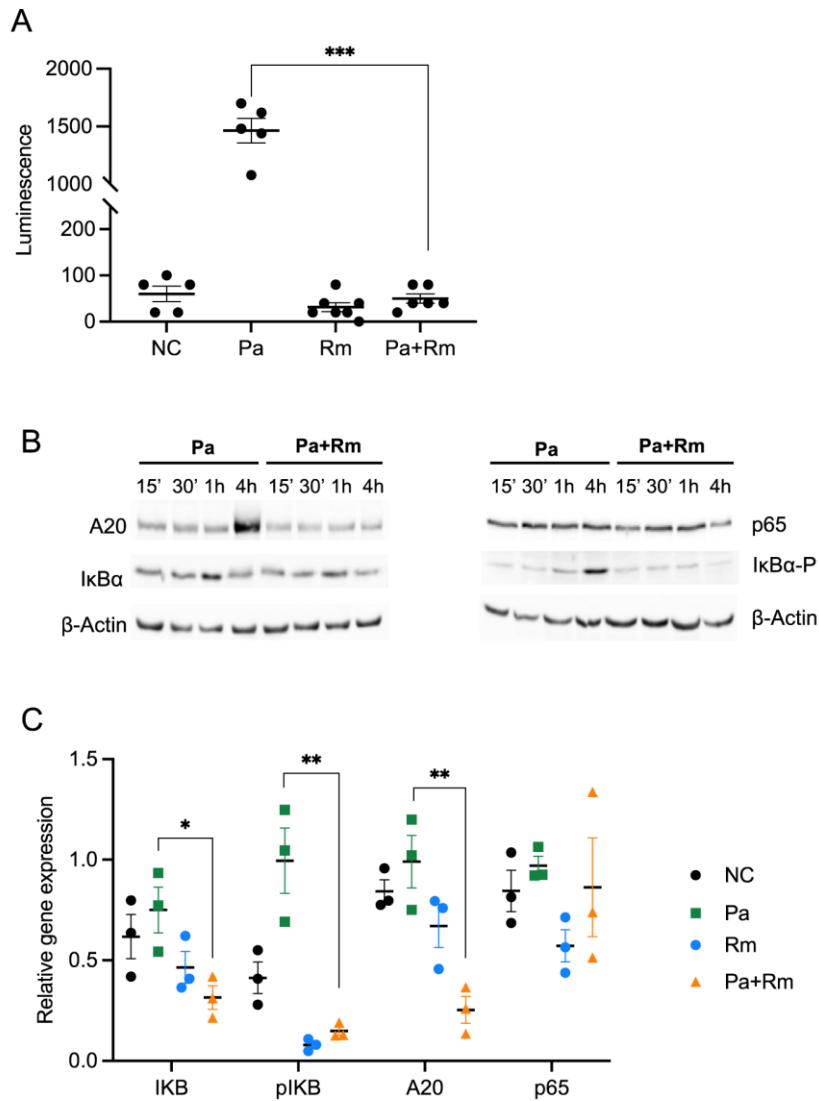


Figure 4. Effect of *R. mucilaginosa* on NF-κB pathway activation by *P. aeruginosa*. (A) Activation of NF-κB pathway measured via luminescence of 3-D NF-κB reporter A549 cells. 3-D cells were exposed for 4 h to *P. aeruginosa* PAO1 alone or in co-culture with *R. mucilaginosa* DSM20746. (B) Semiquantitative determination (by western blotting) of proteins (i.e. A20, IκBα, p65 and P-IκBα) produced by 3-D A549 cells stimulated with *P. aeruginosa* PAO1 with or without *R. mucilaginosa* DSM20746. (C) Band intensity (normalized to β-actin) of Western Blot at 4h of 3-D A549 cells stimulated with *P. aeruginosa* PAO1 with or without *R. mucilaginosa* DSM20746. NC = negative control, uninfected 3-D NF-κB reporter A549 cells in serum-free GTSF-2 medium. Data represent the mean luminescence ± SEM, n=3, *p<0.05, **p< 0.01.

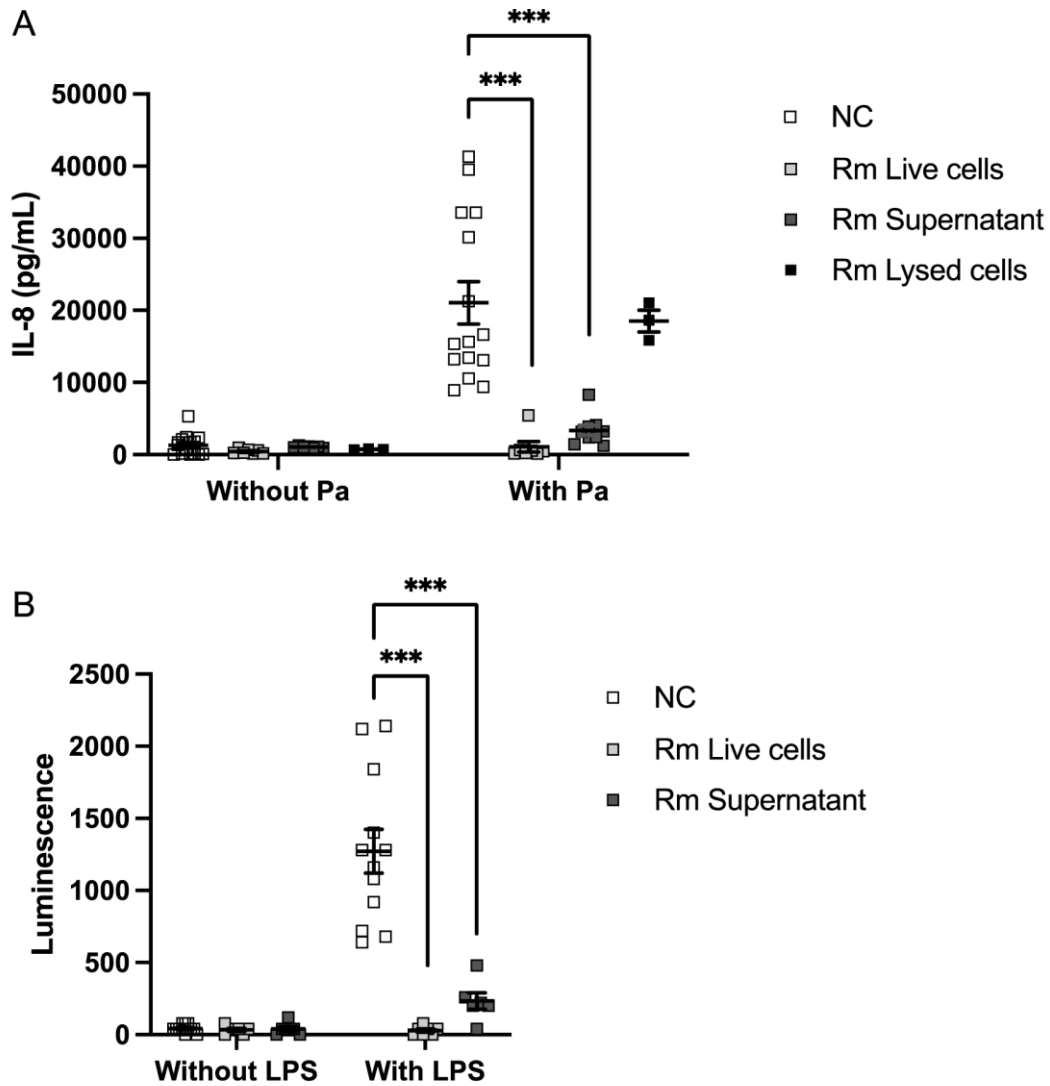


Figure 5. The anti-inflammatory effect of *R. mucilaginosa* is mediated by its cell-free supernatant. (A) IL-8 production by 3-D A549 epithelial cells after exposure to *P. aeruginosa* PAO1 (Pa) for 4h, with or without *R. mucilaginosa* DSM20746 (Rm) live cells, lysed cells or cell-free supernatant. Data represent the mean IL-8 concentration (pg/mL) \pm SEM, $n \geq 3$, $***p < 0.001$. (B) Quantification of NF- κ B pathway activation after 4h exposure to LPS (100 μ g/mL) with or without *R. mucilaginosa* DSM20746 (Rm) cell-free supernatant. Data represent the mean luminescence \pm SEM, $n \geq 3$, $***p < 0.001$. NC= negative control; uninfected 3-D epithelial cells. The MOI was 10:1 in all experiments.

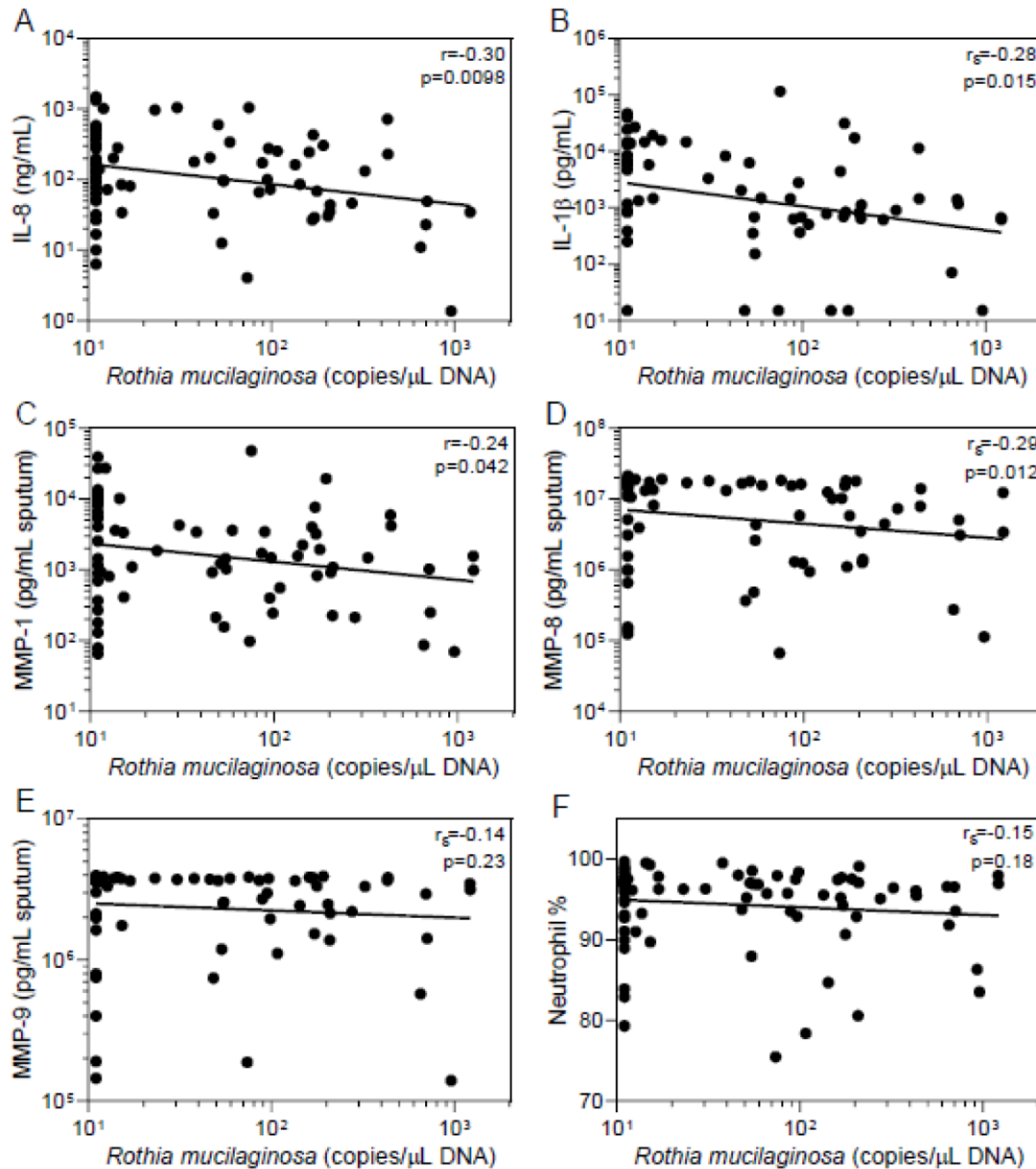


Figure 6. Correlation of absolute load of *R. mucilaginosa* with pro-inflammatory parameters in induced sputum samples from bronchiectasis patients. (A) IL-8 (ng/mL), (B) IL-1 β (pg/mL), (C) MMP-1 (pg/mL), (D) MMP-8 (pg/mL), (E) MMP-9 (pg/mL), (F) % neutrophils. Dots represent individual induced sputum samples. Correlation coefficients and p-values were calculated on ranked values when Spearman's test was used (r_s).

Supplemental figures and legends

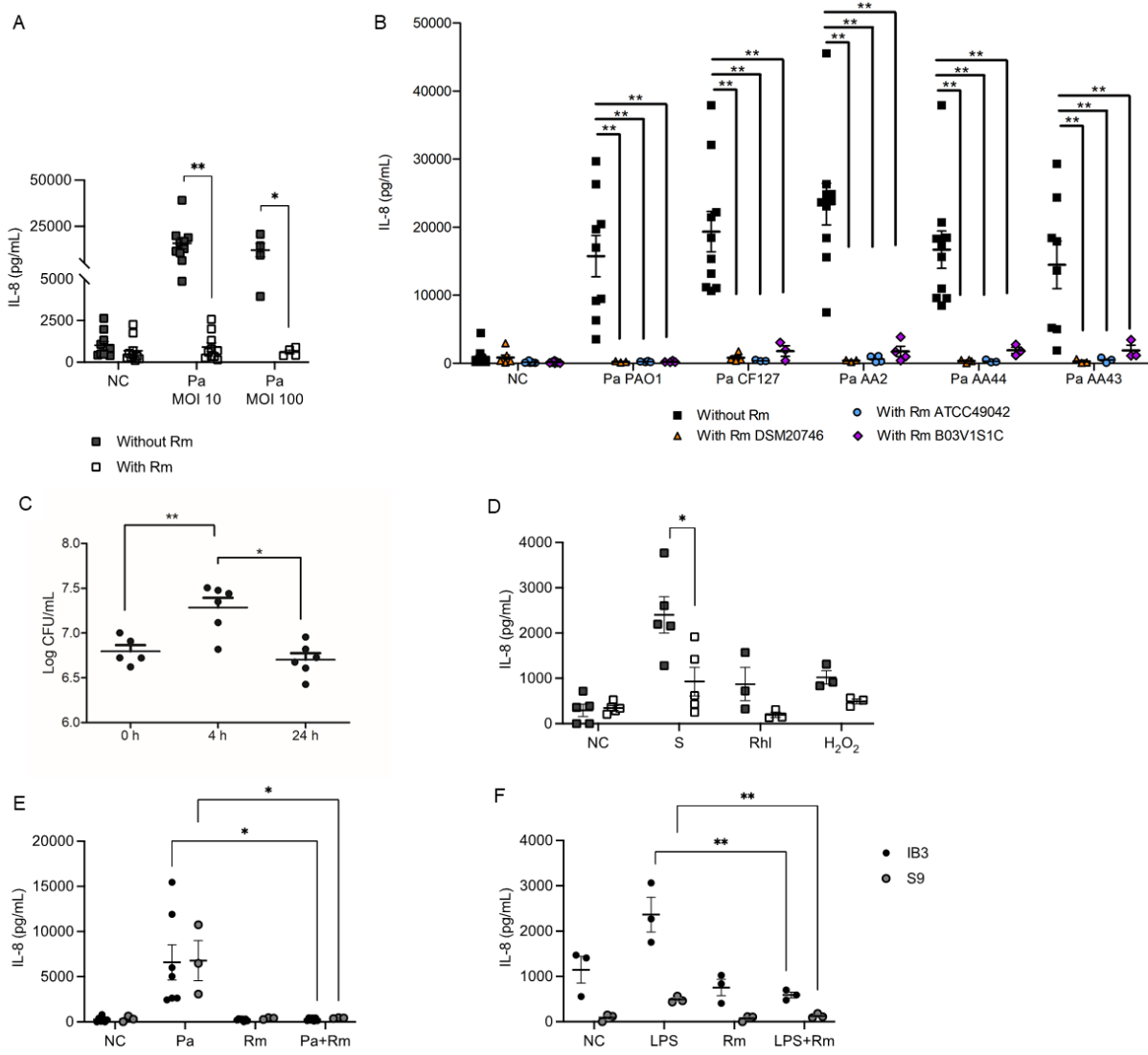


Figure S1. Influence of different *R. mucilaginosa* strains on the pro-inflammatory response of 3-D A549 cells to various *P. aeruginosa* strains and dosages. (A) IL-8 production by 3-D A549 cells after 4h exposure to single *P. aeruginosa* PAO1 culture at various MOI or to co-cultures of *P. aeruginosa* PAO1 with *R. mucilaginosa* DSM20746 at MOI 10:1. (B) IL-8 production by 3-D A549 cells after 4h exposure to various *P. aeruginosa* strains (PAO1, CF127, AA2, AA44, AA43) in single or co-cultures with various strains of *R. mucilaginosa* (DSM20746, ATCC49042, B03V1S1C) at MOI 10:1. (C) CFU/mL of *R. mucilaginosa* DSM20746 at the start of the exposure experiment (inoculum) and after 4h or 24h incubation with 3-D

A549 cells, using an MOI of 10:1. The total CFU/mL, i.e. associated with the 3-D A549 cells and in the surrounding liquid, is presented. (D) IL-8 production by 3-D A549 cells after 4h exposure to various pro-inflammatory stimuli (*S. aureus*, 100 µg/mL LPS, 100 µg/mL rhamnolipid (Rhl), 1 mM H₂O₂) alone or in co-culture with *R. mucilaginosa* at an MOI of 10:1. IL-8 production by 3-D bronchial epithelial CF cells (IB-3) or healthy (CFTR-corrected) 3-D bronchial epithelial cells (S9) after 4h infection with *P. aeruginosa* PAO1 in combination with *R. mucilaginosa* at MOI 10:1 (E) or after 24h exposure to 100 µg/mL LPS in combination with *R. mucilaginosa* at MOI 1:1 (F). Data represent the mean IL-8 concentration (pg/mL) ± SEM, n≥3, *p<0.05, ** p < 0.01

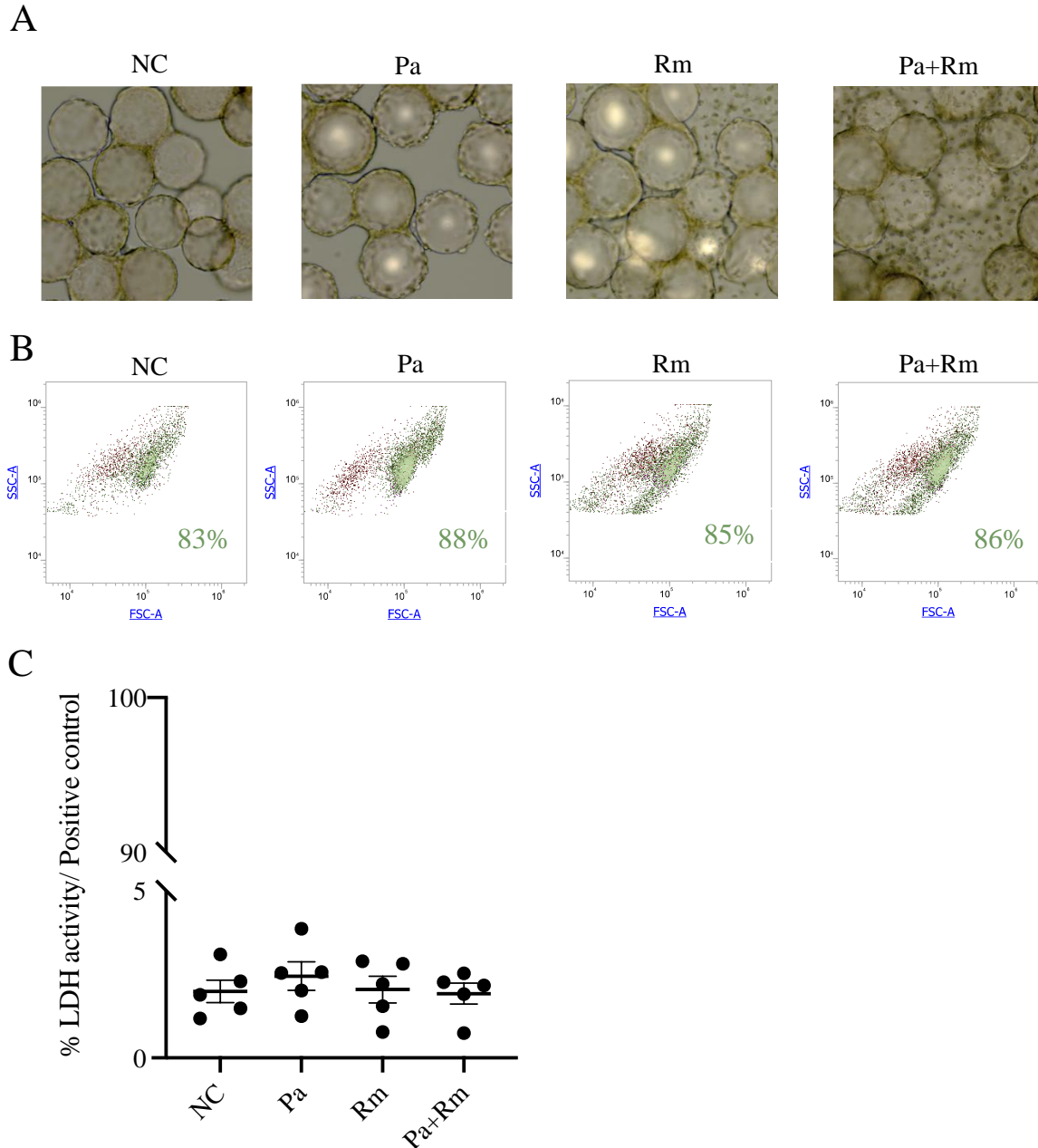


Figure S2. 3-D lung epithelial cell viability. (A) Light microscopy view (276X) of 3-D A549 epithelial cells. Large clusters of *R. mucilaginosa* cells are visible in single (Rm) and mixed (Pa+Rm) culture. (B) Annexin V/PI flow cytometry assay results. Viable cells are displayed in green, dead cells are displayed in red. (C) Percentage LDH activity versus positive control (i.e. lysed 3-D A549 cells). NC = negative control, uninfected 3-D A549 cells in serum-free GTSF-2 medium; Pa = 3-D A549 cells infected for 4 hours with *P. aeruginosa* PAO1; Rm = 3-D A549 cells infected for 4 hours with *R. mucilaginosa* DSM20746; Pa+Rm = 3-D A549 cells infected for 4 hours with a co-culture of *P. aeruginosa* PAO1 and *R. mucilaginosa* DSM20746.

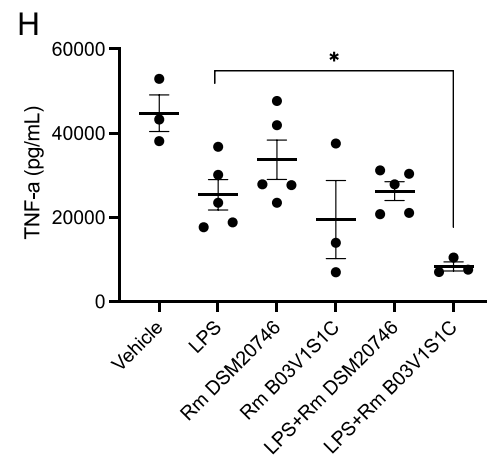
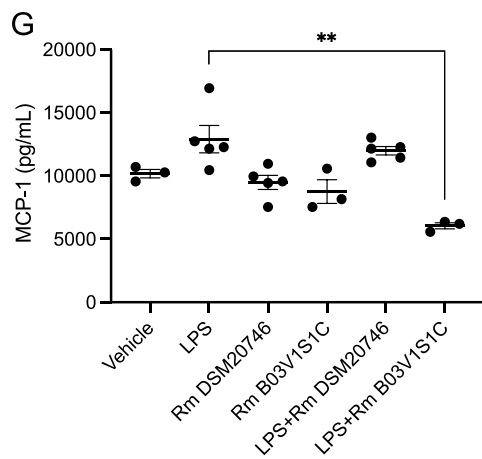
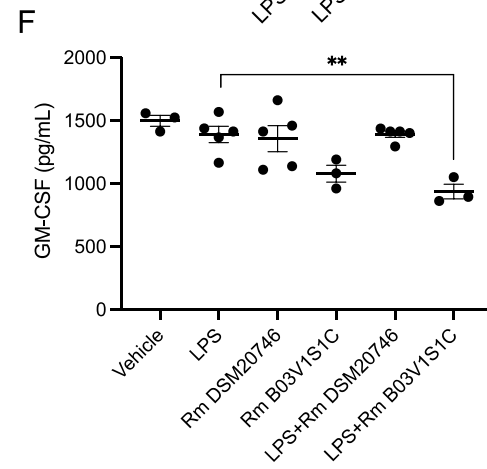
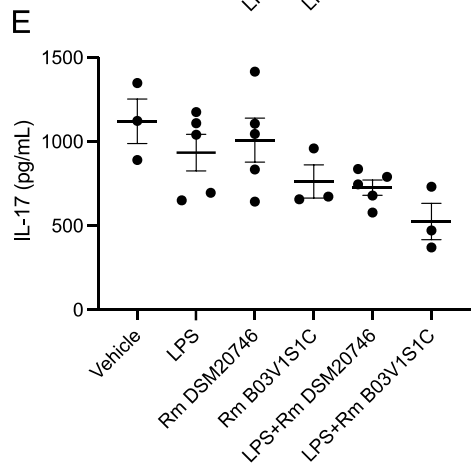
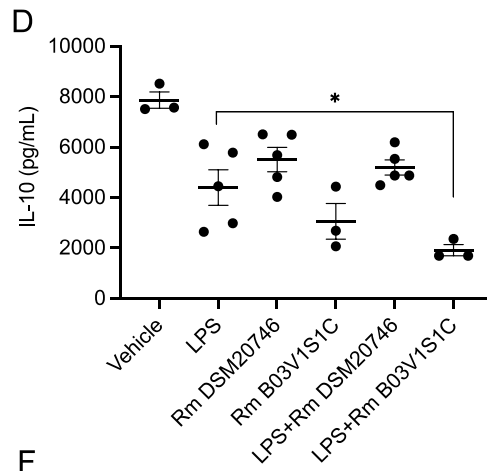
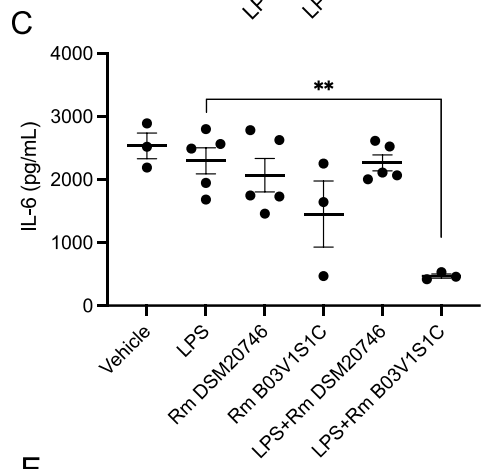
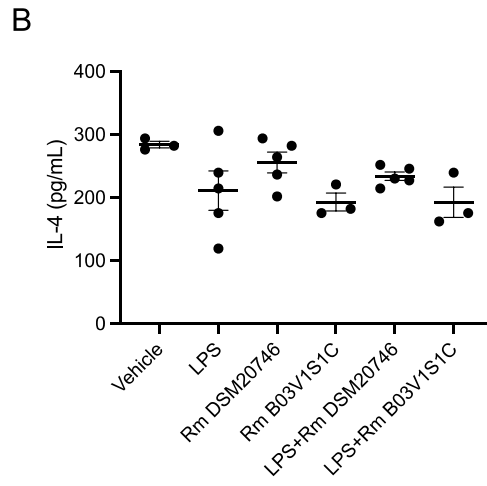
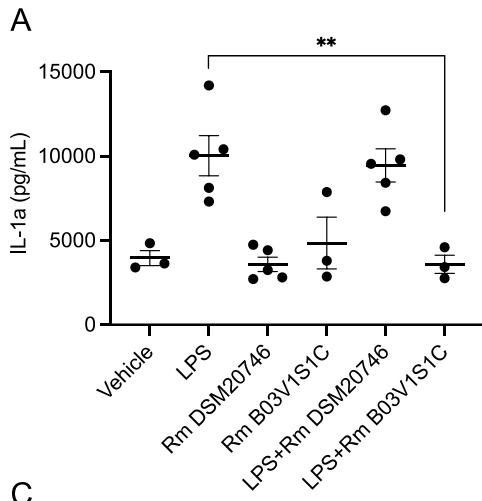


Figure S3. Influence of *R. mucilaginosa* on the *in vivo* cytokine production in response to LPS. Cytokine concentrations (measured by Bioplex) in mice lung homogenates after 48 h exposure to sterile beads (vehicle) (n=3), LPS (n=14), *R. mucilaginosa* suspension (n=5 for *R. mucilaginosa* DSM20746 and n=3 for *R. mucilaginosa* B03V1S1C) or a combination of LPS and *R. mucilaginosa* (n=14 for *R. mucilaginosa* DSM20746 and n=3 for *R. mucilaginosa* B03V1S1C). Data represent the mean cytokine concentration (pg/mL) \pm SEM, n \geq 3, *p<0.05, **p<0.01. Vehicle = sterile alginate beads; LPS = 10 μ g/50 μ L; DSM20746 = *R. mucilaginosa* DSM20746; B03V1S1C = *R. mucilaginosa* B03V1S1C. Data in this figure were obtained in a single animal experiment.

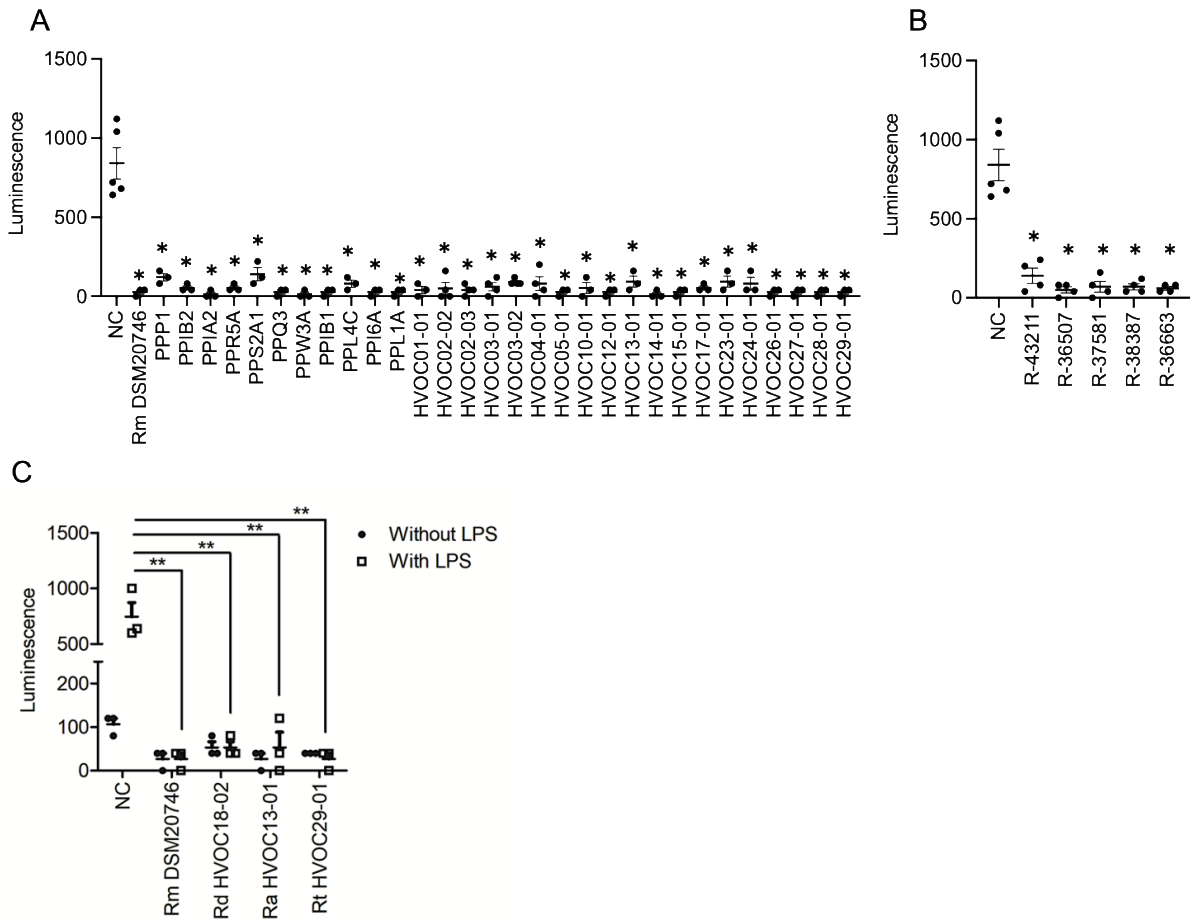


Figure S4. Anti-inflammatory effect of various *Rothia* species. Quantification of NF- κ B activation by (A) *P. aeruginosa* PAO1 alone or in co-culture with various clinical or (B) environmental *Rothia* species or (C) by LPS alone or in co-culture with various *Rothia* species under microaerobic conditions (measured by luminescence of a 3-D A549 reporter cell line). Data represent the mean luminescence \pm SEM, $n \geq 3$, * $p < 0.05$, ** $p < 0.01$ compared to *P. aeruginosa* PAO1 (A, B) or LPS (C).

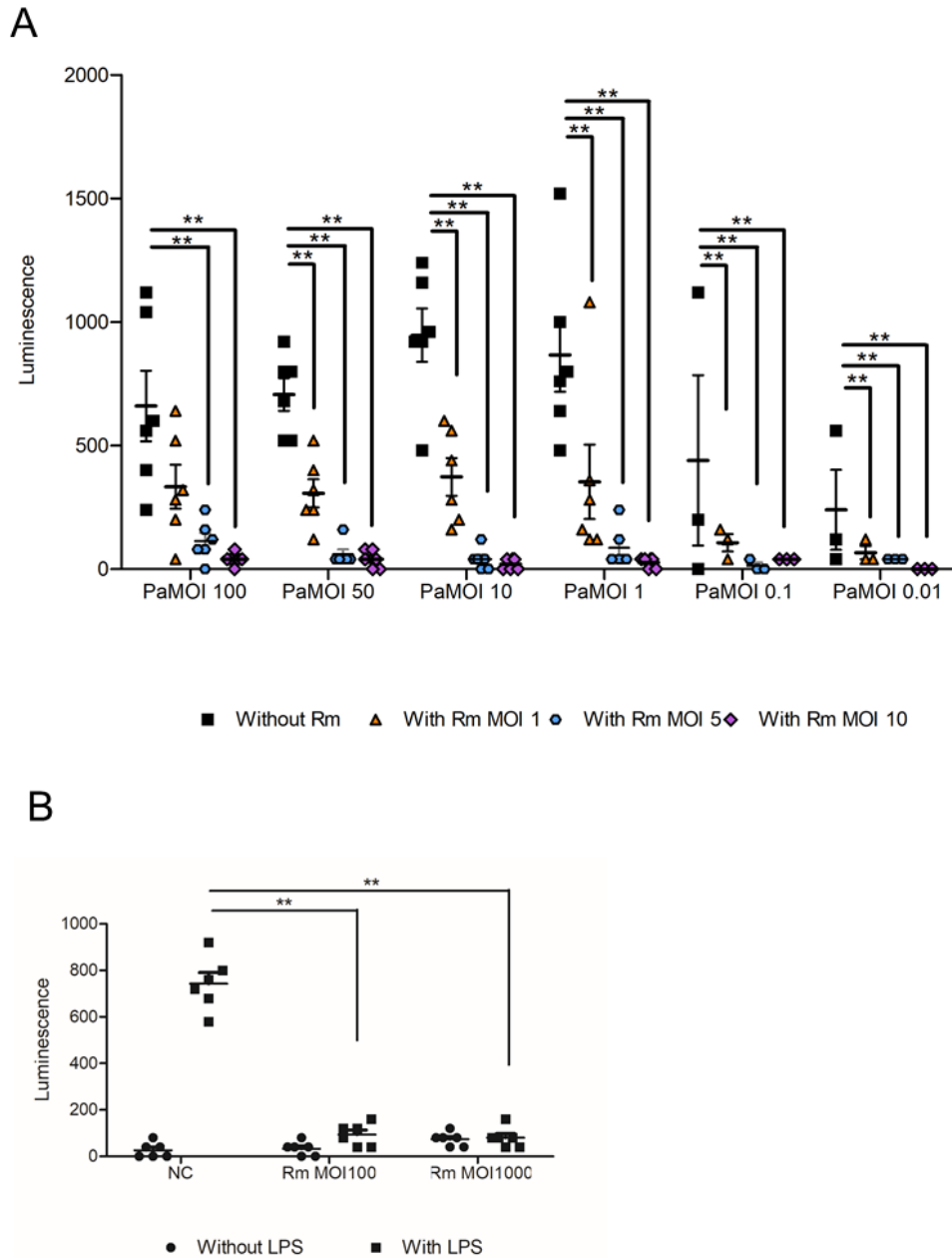


Figure S5. Minimal effective dose of *R. mucilaginosa*. Quantification of NF- κ B activation in 3-D A549 cells (measured by luminescence of a 3-D A549 reporter cell line) after exposure to (A) various MOI of *P. aeruginosa* PAO1 alone or in co-culture with various MOI of *R. mucilaginosa* DSM20746, (B) various MOI of *R. mucilaginosa* DSM20746 with or without LPS. Pa = 3-D A549 cells infected for 4 hours with *P. aeruginosa* PAO1; Rm = 3-D A549 cells infected for 4 hours with *R. mucilaginosa* DSM20746; Data represent the mean luminescence \pm SEM, $n \geq 3$, * $p < 0.05$, ** $p < 0.01$.

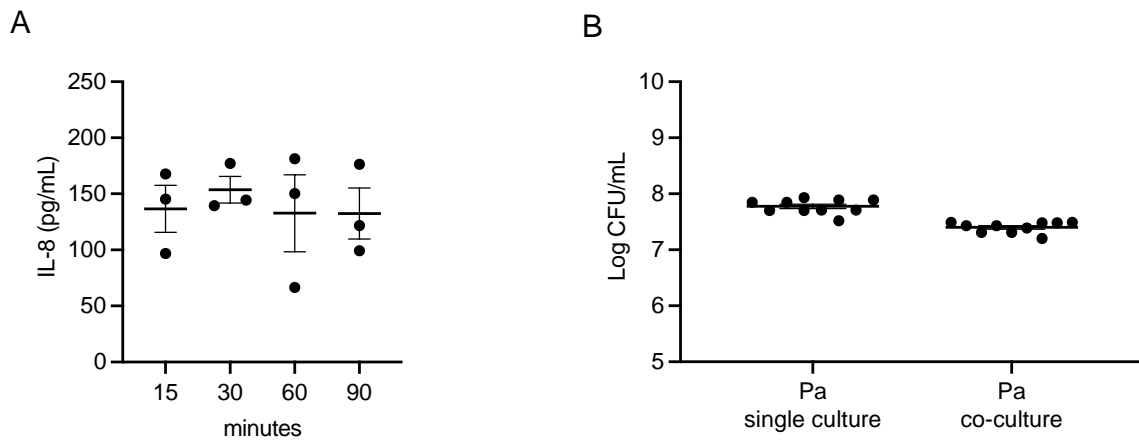


Figure S6. Effect of *R. mucilaginosa* on degradation of IL-8 and PAO1 adhesion to epithelial cells. (A) Concentration (pg/mL) of IL-8 over time after treatment with *R. mucilaginosa* DSM20746. (B) Adhesion (log CFU/mL) of *P. aeruginosa* PAO1 after 4h infection in single culture or in co-culture with *R. mucilaginosa* DSM20746. Data represent the mean IL-8 concentration (pg/mL) and mean Log CFU/mL \pm SEM, $n \geq 3$.

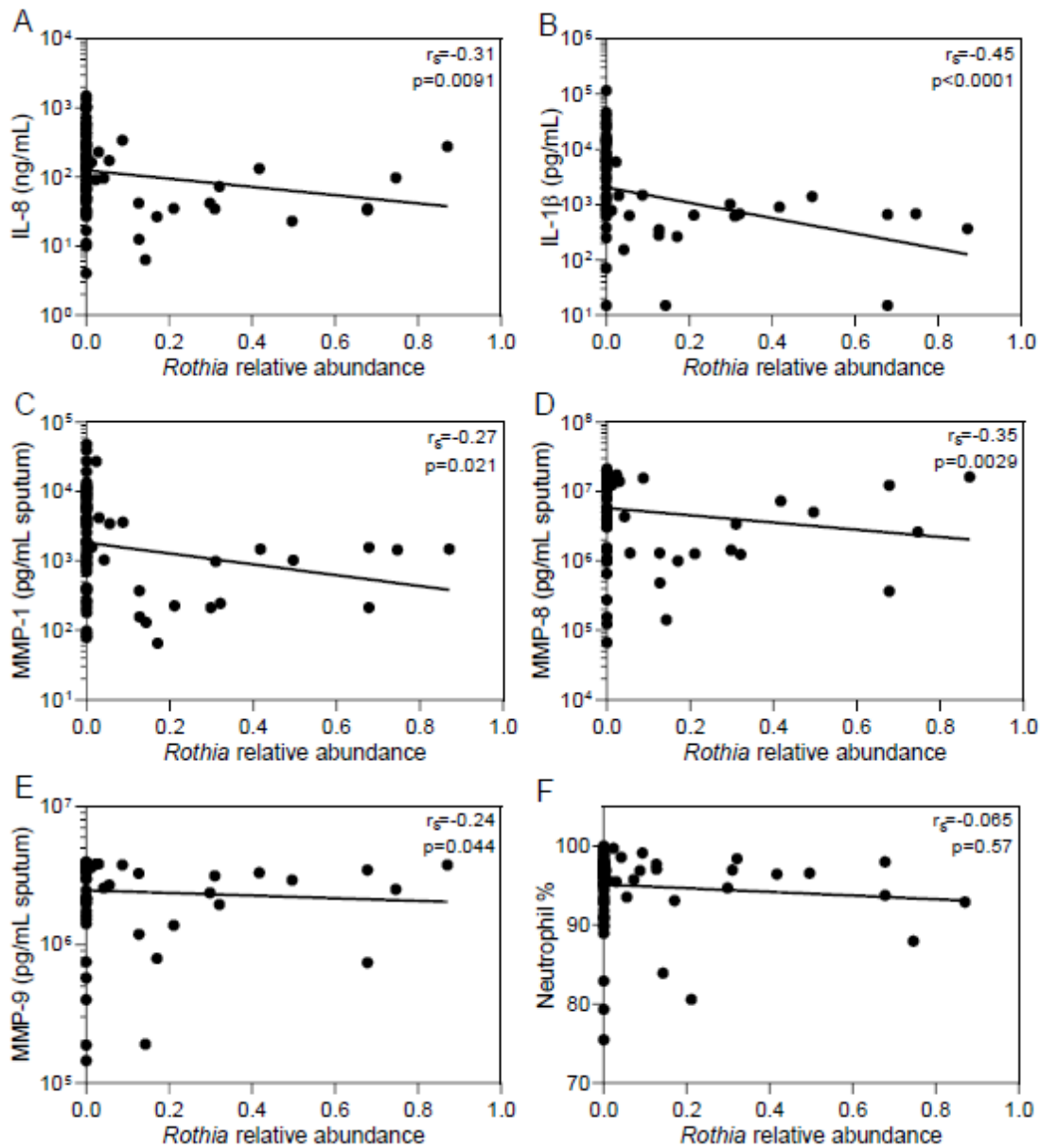


Figure S7. Correlation of relative abundance of *R. mucilaginosa* with pro-inflammatory parameters in induced sputum samples from bronchiectasis patients. (A) IL-8 (ng/mL), (B) IL-1 β (pg/mL), (C) MMP-1 (pg/mL), (D) MMP-8 (pg/mL), (E) MMP-9 (pg/mL), (F) % neutrophils. Dots represent individual induced sputum samples. Correlation coefficients and p-values were calculated on ranked values and determined using a Spearman's correlation analysis.

Supplementary methods

***In vivo* mouse model.** To prepare the inoculum for intratracheal infection, *R. mucilaginosa* cryostock was thawed, incubated in 50 mL falcons with TSB broth for 18 h at 180 rpm and 37 °C. Three independent cultures of 50 mL were pooled to obtain the inoculum. The overnight cultures were centrifuged at 4,750 rpm. The overnight culture was centrifuged at 4,750 rpm. The supernatant was discarded, and 1.2 mL of the pooled pellet was resuspended and embedded in 12 mL of sterile seaweed alginate suspension at 1% filtered through 0.8 µm, 0.45 µm and finally 0.2 µm (Protanal LF 10/60 FT purchased from FMC Biopolymer). The suspension was placed in a 20 mL syringe and forced through a nozzle with a coaxial jet of air blowing to create alginate droplets (Nisco encapsulating unit VarJ30). The alginate droplets were collected in a solution of 0.1 M CaCl₂ Tris-HCl buffer (0.1 M, pH 7.0). After 1 h of stirring, the resulting <30 µm alginate beads were washed twice in 0.9% NaCl with 0.1 M CaCl₂. The number of bacteria embedded in the alginate beads was determined using plate counts on TSA. Before intratracheal challenge, mice were anesthetized with isoflurane (Halocarbon, Norcross, GA) and all efforts were made to minimize suffering. Anesthetized mice were inoculated with *R. mucilaginosa*-containing alginate beads in 50 µL PBS. The negative control consisted of empty beads produced in the same way as described but without bacteria inside, and the positive control (LPS) was added together with empty alginate beads. To evaluate if colonization of mouse lungs with *R. mucilaginosa* was achievable without being embedded in alginate beads, a preliminary experiment was performed using two 7 week old animals. Bacterial cultures were prepared as described above and a dose of 10⁷ CFU/animal (in PBS) was administered intratracheally. Processing of left lungs for CFU determination resulted in colonization of one animal with 5 x 10³ CFU/mL lung homogenate, while 0 CFU/mL could be recovered for the other animal.

Bronchiectasis cohort

Induced sputum samples were obtained from the Bronchiectasis and Low-dose Erythromycin Study (BLESS)[1], corresponding to baseline samples, prior to the trial intervention. Participants had the following inclusion and exclusion criteria and were considered to have moderate to severe bronchiectasis.

Bronchiectasis subject inclusion criteria

1. Able to provide written informed consent.
2. Confirmed diagnosis of bronchiectasis by HRCT within 3 years.
3. Airways obstruction on spirometry (ratio FEV1/ FVC <0.7) and FEV1 \geq 25% predicted.
4. Chronic productive cough with at least 5 mLs sputum production per day.
5. At least two exacerbations of bronchiectasis requiring either oral or intravenous supplemental antibiotic therapy (of at least 7 days on each occasion) in the prior 12 months.
6. Aged 20-85 inclusive.
7. Clinically stable for at least four weeks (defined as no symptoms of exacerbation, no requirement for supplemental antibiotic therapy, and FEV1 within 10% of best recently recorded value where available).

Exclusion criteria

1. Bronchiectasis as a result of CF or focal endobronchial obstruction.
2. Currently active tuberculosis or non-tuberculous mycobacterial (NTM) infection. Subjects with evidence of prior pulmonary NTM infection could be included only if they have completed a course of therapy that is deemed successful on the basis of negative NTM cultures following cessation of therapy. All subjects required a negative NTM culture prior to screening.
3. Any symptoms or signs to suggest recent deterioration in respiratory disease, including exacerbation of pulmonary disease (as previously defined) in the preceding 4 weeks.

4. Any change to medications in the preceding 4 weeks.
5. Prescription of either oral or intravenous antibiotic therapy in the preceding 4 weeks.
6. Cigarette smoking within the preceding 6 months.
7. Any history of malignant arrhythmia (unless in the immediate post-myocardial infarction period and not requiring any regular therapy) or QTc prolongation on baseline ECG.
8. Any of the following within the three (3) months prior to enrolment:
 - Acute MI
 - Acute CVA
 - Major surgery
9. History of any of the following:
 - Active malignancy (excepting non-melanoma skin malignancies that have been treated and considered cured)
 - Listed for transplantation
 - Any other significant active illness likely to affect the patient's survival within 12 months
 - Receiving long-term domiciliary oxygen therapy
10. Allergy to macrolide antibiotics, other than minor, dose-related gastrointestinal intolerance that would not be anticipated to recur with low-dose erythromycin.
11. Any prescription or receipt of long-term macrolide antibiotics, or receipt of a treatment course within 4 weeks.
12. Predominant diagnosis of emphysema (rather than bronchiectasis) on HRCT scan of the chest.
13. Requirement for supplemental oxygen therapy.
14. Inability to complete required study procedures for whatever reason (including 6 minute walk test, hypertonic saline sputum induction).

15. Respiratory symptoms (including cough, sputum production, recurrent exacerbations) not predominantly the result of bronchiectasis in the opinion of the PI; where treatable causes for exacerbations existed, these were treated before considering trial enrolment.

Sputum induction procedure

Subjects were instructed to perform their usual chest physiotherapy regime on the morning of the sputum induction procedure. Prior to commencement of hypertonic saline inhalation, any spontaneous sputum expectorated was collected for standard culture. Sputum induction (SI) was performed after inhalation of 400 ug of albuterol, using 4.5% hypertonic saline nebulised from an ultrasonic nebuliser (output >1 mL/ min) for 20 minutes in 4 periods of 5 minutes each, according to the standardised protocol recommended by the European Respiratory Society taskforce [2]. Following mouth-rinsing and expectoration, sputum was collected following each nebulisation period, on each occasion preceded immediately by spirometry. The first sputum sample was refrigerated immediately following collection and frozen at -80 °C within an hour. A cold chain was maintained up until the point of DNA extraction.

Neutrophils in sputum as a percent of total non-squamous cells

Collected sputum was placed on ice immediately and transferred for processing within 60 minutes. Sputum was processed according to the methods of the US Cystic Fibrosis Therapeutics Development Network Standard Operating Procedure. Briefly, an equal volume of sterile 10% dithiothreitol (DTT) (Sputolysin; Calbiochem- Novabiochem Corp., San Diego, CA), was added to the sputum, then incubated in a shaking water bath at 37°C for 5-10 min, and gently mixed using a transfer pipette at 5-min intervals. A further three times the volume of both DTT and phosphate-buffered saline (Dulbecco's; Gibco BRL, Grand Island, NY) was added and the mixture incubated again in the 37°C shaking water bath for another 5-10 min.

Ten microliters of the homogenized sputum samples, mixed with Trypan Blue, was used to calculate total cell counts, using a standard hemacytometer. A further 0.25-0.50 ml of both samples was used to prepare cytopsin slides for differential cell counts. After staining the slides with Wright's stain, 300 cells were counted and cell differentials calculated.

Pyrosequencing

Bacterial tag-encoded FLX amplicon pyrosequencing (bTEFAP) was performed as reported in a previous publication [3]. Primers: Gray28F 5'-TTTGATCNTGGCTCAG-3' and Gray519r 5'-GTNTTACNGCGGCKGCTG-3') were used to amplify the V1-V3 16S rRNA hypervariable region. Initial generation of the sequencing library involved a onestep PCR of 30 cycles, using a mixture of Hot Start and HotStar high fidelity Taq DNA polymerase. Tag-encoded FLX amplicon pyrosequencing analyses utilized Roche 454 FLX instrument with Titanium reagents, titanium procedures performed at the Research and Testing Laboratory (Lubbock, TX, USA) using RTL protocols (www.researchandtesting.com).

Sequence processing pipeline

The following information is as described in protocol documentation provided by Molecular Research DNA, Texas, USA (www.mrdnalab.com). Custom software written in C# within a MicrosoftH.NET (Microsoft Corp, Seattle, WA, USA) development environment was used for all post sequencing processing. Quality trimmed sequences obtained from the FLX sequencing run were derived directly from FLX sequencing run output files. Tags were extracted from the multi-FASTA file into individual sample-specific files based upon the tag sequence. Tags which did not have 100% homology to the sample designation were not considered. Sequences which were less than 150 bp after quality trimming were not considered. All failed sequence reads, low quality sequence ends and tags and primers were removed. Sequences with

ambiguous base calls, sequences with homopolymers > 6bp were removed, as were any non-bacterial ribosomal sequences and chimeras.

Individual samples were assembled using CAP3 after parsing the tags into individual FASTA files [4]. The ace files generated by CAP3 were then processed to generate a secondary FASTA file containing the tentative consensus (TC) sequences of the assembly along with the number of reads integrated into each consensus. TC were required to have at least 2-fold coverage.

To determine the identity of bacterial species in the remaining sequences, sequences were denoised, assembled into OTU clusters at 97% identity, and queried using a distributed .Net algorithm that utilizes Blastn+ (KrakenBLAST www.krakenblast.com) against a database of high quality 16S rRNA gene bacterial sequences. Using a .NET and C# analysis pipeline the resulting BLASTn+ outputs were compiled, data reduction analysis performed, and sequence identity classification carried out, as described previously [5]. The relative abundance of OTU clusters that align to *Rothia* were extracted and used for analysis.

References

1. Serisier DJ, Martin ML, McGuckin MA, Lourie R, Chen AC, Brain B, Biga S, Schlebusch S, Dash P, Bowler SD. Effect of long-term, low-dose erythromycin on pulmonary exacerbations among patients with non-cystic fibrosis bronchiectasis: the BLESS randomized controlled trial. *Jama* 2013; 309(12): 1260-1267.
2. Paggiaro PL, Chanez P, Holz O, Ind PW, Djukanovic R, Maestrelli P, Sterk PJ. Sputum induction. *The European respiratory journal Supplement* 2002; 37: 3s-8s.
3. Rogers GB, Zain NM, Bruce KD, Burr LD, Chen AC, Rivett DW, McGuckin MA, Serisier DJ. A novel microbiota stratification system predicts future exacerbations in bronchiectasis. *Annals of the American Thoracic Society* 2014; 11(4): 496-503.

4. Huang X, Madan A. CAP3: A DNA sequence assembly program. *Genome research* 1999; 9(9): 868-877.
5. Dowd SE, Wolcott RD, Sun Y, McKeenan T, Smith E, Rhoads D. Polymicrobial nature of chronic diabetic foot ulcer biofilm infections determined using bacterial tag encoded FLX amplicon pyrosequencing (bTEFAP). *PloS one* 2008; 3(10): e3326.